Bioorganic Chemistry 86 (2019) 583–597

Contents lists available at ScienceDirect

Bioorganic Chemistry

journal homepage: www.elsevier.com/locate/bioorg

Ligand based design and synthesis of pyrazole based derivatives as selective COX-2 inhibitors

Manikanta Murahari[a], Vivek Mahajan[b], Sreenivasulu Neeladri[b], Maushmi S. Kumar[c], Y.C. Mayur[c,*]

[a] Pharmacological Modelling & Simulation Centre, M.S. Ramaiah University of Applied Sciences, Bangalore 560 054, India
[b] Medicinal Chemistry Research Division, VL College of Pharmacy, Raichur 584103, India
[c] Department of Pharmaceutical Chemistry, SPP School of Pharmacy & Technology Management, SVKM's NMIMS, Mumbai 400 056, India

ARTICLE INFO

Keywords:
Pyrazole
NSAIDs
COX-2
Anti-inflammatory
Ligand based design
Pharmacophore

ABSTRACT

The design and synthesis of novel pyrazole based derivatives has been carried out using the ligand based approach like pharmacophore and QSAR modelling of reported pyrazoles from the available literature to investigate the chemical features that are essential for the design of selective and potent COX-2 inhibitors. Both pharmacophore and QSAR models with good statistical parameters were selected for the design of the lead molecule. Also by exploiting the chemical structures of selective and marketed COX-2 inhibitors, celecoxib and SC-558 were used in designing the molecules which are used in the treatment of inflammation and related disorders. The therapeutic action of the Non-Steroidal Anti-inflammatory Agents (NSAIDs) is based primarily on the COX-2 inhibition. With this background we have synthesized some azomethine derivatives of 3-methyl-1-substituted-4-phenyl-6-[{(1E)-phenylmethylene}amino]-1,4-dihydro pyrano[2,3-c]pyrazole-5-carbonitrile **6(a-o)** and were characterized by ^{1}HNMR, ^{13}CNMR and Mass spectral techniques. All the synthesized pyrazole derivatives were tested for *in vitro* membrane stability property in both COX-1 & COX-2 inhibition studies and *in vivo* anti-inflammatory activity by carrageenan induced rat paw edema model. Among them, compound **6k** showed very good activity by *in vivo* anti-inflammatory activity with 0.8575 mmol/kg as ED_{50}. Similarly compounds **6m, 6o, 6i** and **6h** exhibited comparable anti-inflammatory activity to standard drugs. Also the active compounds were further screened for ulcerogenic activity and were found be safer with less ulcer index compared to the marketed drugs like aspirin, ibuprofen and celecoxib.

1. Introduction

Most of the currently used non-steroidal anti-inflammatory drugs (NSAIDs) show severe side effects and majority of these drugs showing gastrointestinal and renal toxicity [1,2]. There has been a continuous interest among researchers in discovering newer NSAIDs which are selective to cyclooxygenase-2 (COX-2) enzyme. Unrelated and non-specific side effects exerted by the classical NSAIDs is due to inhibition of physiologically important cyclooxygenase-1 (COX-1) enzyme [3]. Isozyme COX-2 is more responsible for the release of prostaglandins as inflammatory mediators [4,5]. The heterocyclic class of compounds have been studied widely as a new class of NSAIDs with lesser gastric side effects, a new series of compounds were synthesized with a focus to develop safer drugs [6]. Pyrazole derivatives are well established heterocyclic systems with established biological significance, safe and effective drugs used therapeutically. Feasible synthetic routes and conjugation with diverse aromatic and heterocyclic rings are subjected in many research investigations of varied pharmacological profiles such as anti-inflammatory, antipyretic, antimicrobial, antiviral, antitumor, anticonvulsant, antihistaminic, and antidepressant activities [6–8]. The pyrazole scaffold is a well-known and widely explored for anti-inflammatory activity by many research groups [9–14]. Most commonly prescribed NSAIDs which are pyrazole based derivatives like celecoxib, deracoxib, etc., are selective and potent COX-2 inhibitors [15,16].

In view of above mentioned findings, authors have utilized the strength of pharmacophore modelling to investigate the structural features of pyrazole derivatives required to selectively inhibit COX-2 enzyme. In addition to that, we have used pyrazole derivatives celecoxib, SC-558 and antipyrine (2,3-dimethyl-1-pheny-3-pyrazolin-5-one) one of the first identified pyrazolone derivative prescribed and suggested in the management of pain and inflammation. The drug Antipyrine was withdrawn because of its toxicity, but due to its

* Corresponding author at: Department of Pharmaceutical Chemistry, SPPSPTM, SVKM's NMIMS University, Vile Parle (West), Mumbai 400 056, India.
E-mail address: mayuryc@rediffmail.com (Y.C. Mayur).

https://doi.org/10.1016/j.bioorg.2019.02.031
Received 4 January 2019; Received in revised form 6 February 2019; Accepted 12 February 2019
Available online 14 February 2019
0045-2068/

potential activity their derivatives have enticed the attention of researchers across the globe [17–19]. Further, we employed the most advanced Auto Quantitative Structure Activity Relationship (Auto-QSAR) tool to build a model of experimentally reported pyrazoles which are selective COX-2 inhibitors to quantify the therapeutic potential of synthesized pyrazoles. In continuation of our previous study and to explore the potential of new candidates which are selective and less toxic anti-inflammatory agents, we are reporting the ligand based design and synthesis, evaluation by *in vitro* and *in vivo* methods for anti-inflammatory activity of novel pyrazole derivatives [20]. Also the ulcerogenic activity has been carried out to check the gastric related side effects of these drugs.

2. Results and discussion

2.1. Generation of ligand based pharmacophore model

Pharmacophore model of pyrazole derivatives have been generated with 7 active (pIC_{50} greater than 6.30) and 11 inactive compounds (pIC_{50} < 4.35) from selective COX-2 inhibition assay results. Other compounds pIC_{50} which were in the range of 4.35–6.30 were considered as moderately active. All the compounds were screened for selective COX-1 and COX-2 inhibition assay and identified that substituted pyrazoles were selective to COX-2 enzyme with a pIC_{50} values in the range of 4.3010–6.5376. The trail run could generate two five point and nine four point hypothesis respectively with all active ligands matching the pharmacophoric features. The parameters listed were generated by the Phase module and AHHR_1 was nominated as best hypothesis for screening and identification of selective COX-2 inhibitors (Supplementary Data). The model AHHR_1 was characterized by survival score of 4.782, inactive score of 2.481 and selective score of 1.380. The hypothesis represents that one hydrogen bond acceptor, two hydrophobic groups and one aromatic ring at a specific spatial arrangement of angstroms (Å) highlighted in Fig. 1 are crucial for the selective COX-2 inhibition. Hypothesis results for pyrazole derivatives are shown (Supplementary Data).

2.2. Validation of pharmacophore model

To investigate the predictability of AHHR_1, enrichment view was reviewed for all the hypotheses. The selected hypothesis AHHR_1 was found with highest Phase Hypo Score of 1.29, AOC and ROC values as 1 with all seven active compounds matched 4 features of hypothesis (Fig. 2). Interestingly plot generated by Phase for AHHR_1 hypothesis suggests that model can filter 100% of active molecules from the database screening with true positive rate (Fig. 2). To further validate the efficiency and selectivity of COX-2 inhibitors hypothesis, a model was screened with two data sets i.e., one external test set of selective COX-2 inhibitors and standard drugs. One data set included 12 compounds which were evaluated for COX-1 & 2 enzyme inhibition assay and *in vivo* anti-inflammatory activity by the same biological method. Another data set of standard drugs in market and clinical investigation as non-selective and selective COX-2 inhibitors. Both the datasets were screened through hypothesis and results are shown (Supplementary Data). Hypothesis screening of 12 compounds were found in correlation with experimental results. Experimental results indicated that all 12 compounds were selective to COX-2 inhibition and pIC_{50} was observed in the range of 4.337–6.347. All the 12 compounds matched four sites of hypothesis and interestingly most active and inactive compounds have highest and least Phase score (Supplementary Information). The

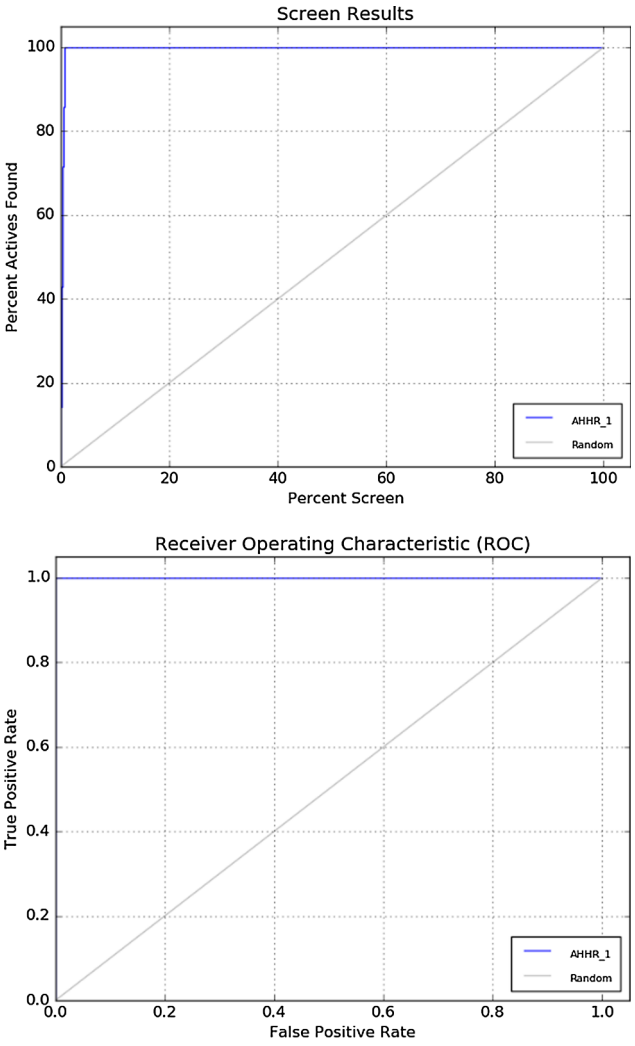

Fig. 2. Percentage screen and ROC plot AHHR_1.

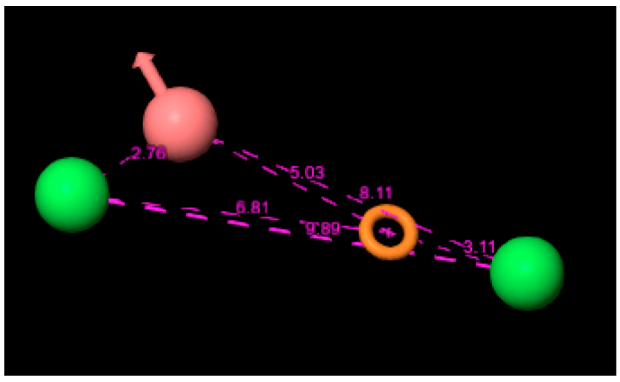

Parameter	Value
Survival Score	4.782
Inactive Score	2.481
Site Score	0.975
Vector Score	0.955
Volume Score	0.627
Selectivity Score	1.380

Fig. 1. Pharmacophore model of COX-2 Inhibitors AHHR_1-Acceptor (A), Hydrophobic (H), Aromatic ring (R) with statistical data of hypothesis.

Table 1
Validation of Pharmacophore Model with Standard Drugs.

Non-selective COX Inhibitors	S. No.	Drug Name	Matched ligand sites	Fitness score	Vector score	Volume score
	1	Aspirin	No sorted hits for match of at least 3 out of 4 features			
	2	Ibuprofen				
	3	Flurbiprofen				
	4	Naproxen	3	1.398	0.654	0.397
	5	Indomethacin	4	1.831	0.892	0.622
	6	Diclofenac	No sorted hits for match of at least 3 out of 4 features			
	7	Mefenamic acid				
	8	Piroxicam				
Selective COX-2 Inhibitors	9	DuP-697	4	1.265	0.907	0.325
	10	SC-558	4	2.558	0.998	0.622
	11	Celecoxib	4	2.538	0.998	0.621
	12	Valdecoxib	3	2.007	0.997	0.524
	13	Parecoxib	3	1.960	0.997	0.477
	14	Rofecoxib	3	1.637	0.983	0.439
	15	Etoricoxib	4	2.169	0.989	0.442
	16	Lumiracoxib	3	1.684	0.906	0.404

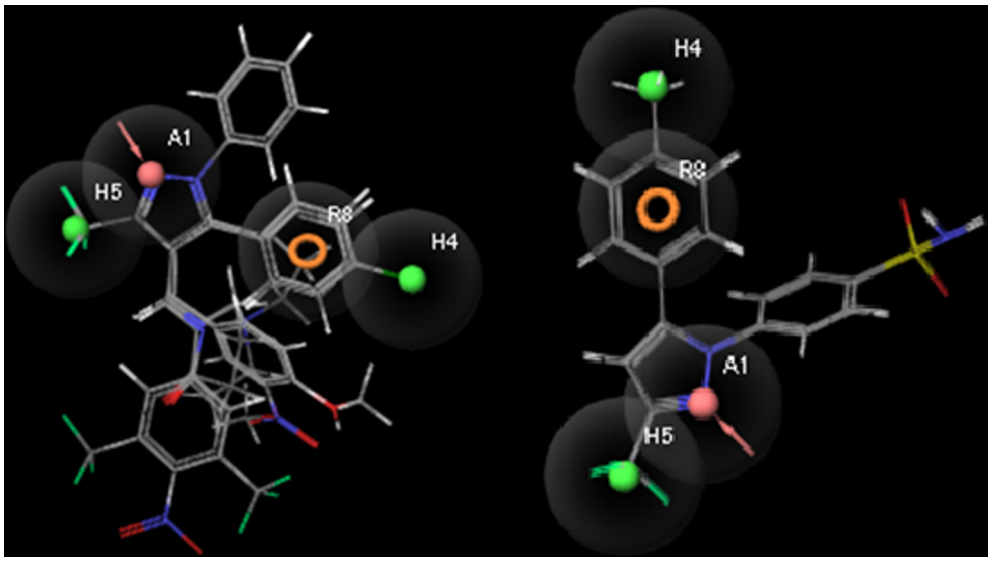

Fig. 3. (a) Seven Active pyrazoles with pIC_{50} greater than 6.30 aligned with pharmacophore AHHR_1 and (b) Standard drugs SC-558 and Celecoxib aligned with pharmacophore AHHR_1.

nominated hypothesis AHHR_1 has good results accomplished by selectively screening the COX-2 inhibitor drugs and leaving the non-selective COX inhibitor molecules. The model suggests that naproxen and indomethacin were selective to COX-2 enzyme inhibition. All the selective COX-2 inhibitors have displayed good scores highlighting Celecoxib and SC-558 with highest fitness score of 2.558 and DuP-697 as least with 1.265 (Table 1). Interestingly both the drugs are of congeneric series sharing pyrazole as common nucleus (Fig. 3). With respect to screening of drugs i.e., 8 of non-selective COX as inactive and 8 of selective COX-2 as active inhibitors through pharmacophore model, the sensitivity is 1.25 and specificity is 0.75.

2.3. Auto QSAR statistical results

A congeneric series of 25 pyrazole derivatives were collected from the literature and randomly categorized as training and test sets in the ratio of 80:20. Trial run of Quantitative Structure Activity Relationship (QSAR) generated different models and were arranged in ranking order based on statistical values calculated by Auto QSAR tool of Schrodinger Drug Design Suite. The best model that identified was based on the values of R^2, Q^2, Standard deviation and Root Mean Square Error (RMSE). Study could identify model of KPLS molprint 2D principle with R^2 and Q^2 values of 0.7711 and 0.7233 respectively. Also standard deviation and RMSE values were observed as 0.4578 and 0.4991 respectively. The effectiveness and accuracy of the model can be explained with small deviation from R^2 and Q^2 values. Predicted pIC_{50} values of pyrazoles from literature with deviation or error from experimental pIC_{50} is shown in Table 2. Also it has been graphically represented to understand that the deviation between experimental and predicted pIC_{50} values in Fig. 4. The following kpls_ molprint2D_45 was selected as best model for prediction of biological activity of unknown compounds.

2.4. Design of substituted pyrazole derivatives as selective COX-2 inhibitors

Pharmacophore modelling of substituted pyrazoles as selective COX-2 inhibitors identified from the literature demonstrated that one hydrogen bond acceptor, two hydrophobic groups and one aromatic ring are essential. Further validation of model with drugs in market and clinical investigation as selective COX-1 and COX-2 inhibitors, pharmacophore model could selectively identify COX-2 inhibitors and concluded SC-558 and celecoxib with highest fitness score. Considering the structural features of both the drugs and essential pharmacophoric features for selective COX-2 inhibition, we have made an effort to synthesize a series of fifteen pyrazole derivatives (Fig. 5). The common trifluoromethyl group of both the drugs was replaced with a nitrile to investigate the significance on anti-inflammatory activity. Many new chemical entities (NCEs) containing nitrile group are currently under

Table 2
QSAR Results of Pyrazoles Collected from Literature.

Best QSAR Model = kpls_molprint2D_45
Ranking score = 0.668606

Training set- 20 compounds (80%)	Standard deviation		0.4578
Test set- 5 compounds (20%)	R^2		0.7711
	RMSE		0.4991
	Q^2		0.7233

S. No.	Compound code	Pharma set	pIC50 (experimental)	pIC50 (predicted)	Error
1	1.3a	Training	4.3468	4.0381	−0.3086
2	1.3b	Test	4.3979	4.2699	−0.1281
3	1.3c	Training	5.5229	4.4973	−1.0256
4	1.3d	Training	4.3468	4.4396	0.0928
5	1.3e	Training	4.3468	4.1304	−0.2164
6	1.3f	Test	4.3468	4.2699	−0.0769
7	1.5	Training	6.2596	5.5614	−0.6982
8	1.6a	Training	6.3468	5.9083	−0.4385
9	1.6b	Training	4.3468	4.9543	0.6076
10	1.6c	Training	5.0000	5.4238	0.4238
11	1.6d	Training	6.3468	6.0662	−0.2806
12	1.6e	Training	4.3468	4.3604	0.0136
13	1.6f	Training	4.3468	4.3604	0.0136
14	2.3a	Training	4.3526	4.8804	0.5277
15	2.3b	Training	6.3188	6.5532	0.2344
16	2.3c	Test	5.6778	5.6863	0.0085
17	2.3d	Training	6.5376	6.7142	0.1766
18	2.3e	Test	6.3665	5.9012	−0.4653
19	2.3f	Training	4.3188	4.5009	0.1822
20	2.5	Training	4.3010	4.4985	0.1975
21	2.8a	Training	5.4949	5.8253	0.3304
22	2.8b	Training	4.3098	4.8262	0.5164
23	2.8c	Training	6.3872	5.7719	−0.6153
24	2.8d	Test	6.5850	5.5818	−1.0033
25	2.9	Training	4.3010	4.5677	0.2667

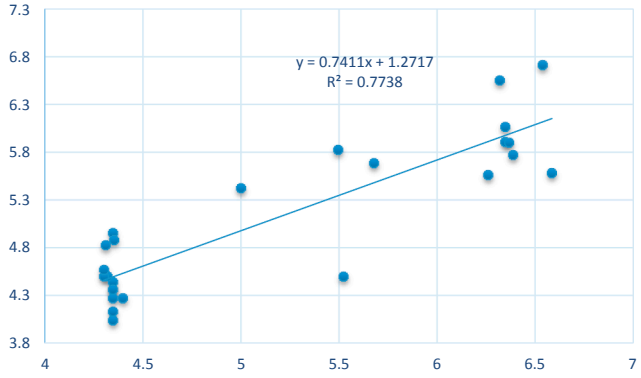

Fig. 4. Plot of COX-2 Inhibition pIC_{50} (experimental) vs pIC_{50} (predicted) for pyrazole derivatives from literature.

clinical investigation emphasizing the safety and potency of substitution. In addition to structural advantages, literature suggests that nitrile groups containing compounds will not be metabolized readily, have improved binding affinity towards the target and also release of cyanogen was not observed [21].

2.5. Chemistry

The starting material, unsubstituted\substituted 3-methyl-1-pyrazole-5-ones (**2a,b**) were prepared from ethylacetoacetate (**1**) and hydrazine hydrate\phenyl hydrazine in one step in good yields. The structure of the compounds (**2a,b**) were confirmed by spectral data (IR, ^{1}HNMR, MS). ^{1}HNMR spectrum of **2a** showed δ = 7.1–7.9 ppm (m, 5H, Ar-H), compounds (**2a,b**) showed δ = 2.0–2.1 ppm (s, 3H, $-CH_3$). The IR spectrum of compound showed characteristic absorption band at ν = 1790 cm^{-1}, 1807 cm^{-1} for CO, 3030 cm^{-1} correspond to aromatic C—H stretching. Mass spectrum showed the prominent ion peak at *m/z* 99 and 175 (M + 1) respectively. The 3-methyl-1-unsubstituted\substituted pyrazole-5-ones (**2a,b**) were converted into 6-amino-3-methyl-1-substituted-4-phenyl-1,4-dihydropyrano[2,3-c]pyrazol-5-carbonitriles (**4a-o**) by reacting with different aromatic aldehyde (**3**), malononitrile and by using alcohol medium in the presence of piperidine by stirring for 2 h at room temperature. The ^{1}HNMR spectrum of the compounds showed δ = 5.6–5.7 ppm (s, 1H, H of pyran), 2.3–2.5 ppm (s, 3H, $-CH_3$). In the 3rd step the 6-amino-3-methyl-1-substituted-4-phenyl-1,4-dihydropyrano[2,3-c]pyrazole-5-carbonitrile (**4a-o**) were converted to respective azomethines by refluxing for 3 h with aromatic aldehydes (**5**) in alcoholic medium by using glacial acetic acid as catalyst, which yields 3-methyl-1-substituted-4-phenyl-6-[{(1E)-phenylmethylene}amino]1,4-dihyropyrano[2,3-c] pyrazole-5-carbonitrile (**6a-o**) as per Scheme 1. All the intermediates were recrystallized and final pyrazoles derivatives were purified by column chromatography, purity was checked by HPLC and chemical structures were interpreted and confirmed by ^{1}HNMR, ^{13}CNMR, Mass and IR spectroscopy techniques (Table 3).

2.6. Biological activity

The main classical mechanism of anti-inflammatory drugs is mediated by inhibition of prostaglandins (PG) synthesis by cyclooxygenase enzyme [22]. The action of the enzyme in the conversion of prostaglandin G2 (PGG2) to PGH2 along with peroxidation is associated with formation of long channels in membranes. The channel opening occurs due to discharge of chemical mediators and so arachidonic acid is released from membrane and transformed to prostaglandin. The extracellular activity of these enzymes is said to be related to acute and chronic inflammation. The action of NSAIDs is either by hindering these lysosomal enzymes (cyclooxygenase) or by stabilizing the lysosomal membrane [23,24]. A series of pyrazole derivatives were prepared and

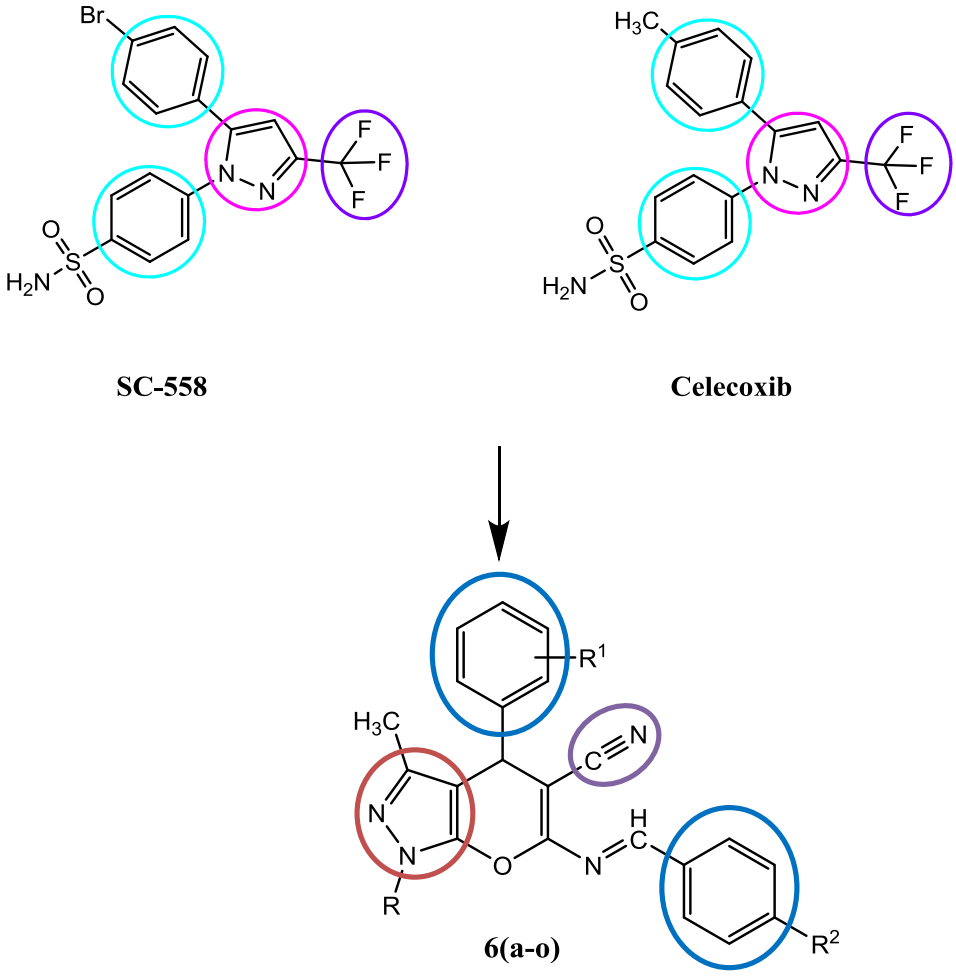

Fig. 5. Design approach of pyrazoles as selective COX-2 Inhibitors.

evaluated for *in vitro* Cyclooxygenase inhibition assay, HRBC membrane stabilizing method and *in vivo* anti-inflammatory activity by mercury displacement method using carrageenan rat paw edema model.

2.6.1. In vitro membrane stabilizing property [25–28]

The *in vitro* anti-inflammatory activity results (Table 4) indicated that all the compounds (**6a-o**) at the concentration of 1 mg/ml exhibited moderate to significant anti-inflammatory activity in HRBC membrane stabilization method. The standard drug Celecoxib and Ibuprofen has demonstrated 72 and 75% of membrane stability. The compounds **6e** and **6o** with 4-fluoro substitution exhibited 71.12% and **6c** with 2-nitro substitution showed 70.15% membrane stabilization comparable to the standard drug. Similarly, compounds substituted with halogen (i.e., chloro at 2nd position) **6d** and **6m** have displayed good stabilization of 69.97 and 67.60% respectively. Surprisingly compounds **6l** with nitro group at 3rd position has curiously reduced the activity to 55.15% and was found to be least among all the compounds. Also compound **6n** with 3-chloro has diminished the activity to 56.12%. Substitution of compounds with electron donating groups like hydroxyl and mono, -di, -tri methoxy groups have reduced the membrane protection. The unsubstituted compound **6f** exhibited stabilization of 59.55% indicating the significance of substitution of phenyl ring for the activity.

2.6.2. In vivo anti-inflammatory study

The *in vivo* anti-inflammatory activity results indicated that all synthesized pyrazole derivatives **(6a-o)** when tested at a dose of 200 mg/kg exhibited considerable *in vivo* activity in acute inflammatory models induced by carrageenan in rats. The edema volume of pyrazoles (**6a-o**) and standard drug ibuprofen and celecoxib are shown in Table 4. In addition to that, ED_{50} values of all the compounds and standard drugs in mg/kg and mmol/kg were determined using Graphpad Prism from percentage reduction in volume with respect to time (Table 6) [29,30]. Standard drugs Ibuprofen and Celecoxib have demonstrated ED_{50} values of 4.606 and 3.060 mg/kg respectively. Selective COX-2 inhibitor celecoxib has exhibited potential anti-inflammatory activity compared to non-selective inhibitor ibuprofen. Compounds have exhibited percentage reduction of edema volume in the range of 21.42–33.57% after 4th hr and ED_{50} in the range of 0.8575–1.404 mmol/kg. All the pyrazoles have displayed moderate activity and the compounds **6k** and **6m** showed the highest *in vivo* anti-inflammatory activity at concentration of 0.8575 and 0.9254 mmol/kg as ED_{50}. Much differences were not observed in the paw edema volume of compounds (**6a-o**). Similarly, **6e** and **6j** were found to be less active at concentration of 1.2466 and 1.404 mmol/kg among all the compounds.

Observing the Structure Activity Relationship (SAR) of synthesized pyrazoles (**6a-o**), compounds substituted with electron with-drawing groups like nitro at 2nd position (**6k**), halogens like chlorine at 2nd (**6m**) and fluoro at 4th position (**6o**) have potentiated the activity. Interestingly, five compounds i.e., **6i, 6h 6k**, **6m** and **6o**, have exhibited $ED_{50} < 1$ mmol/kg revealed that unsubstituted phenyl ring is directly linked to nitrogen of pyrazole might be essential for complementary stacking interactions with amino acids at the active pocket of COX-2 is benefiting the actual inhibition. In the series of pyrazoles from (**6a-e**), unsubstituted pyrazoles especially lacking phenyl ring have greatly

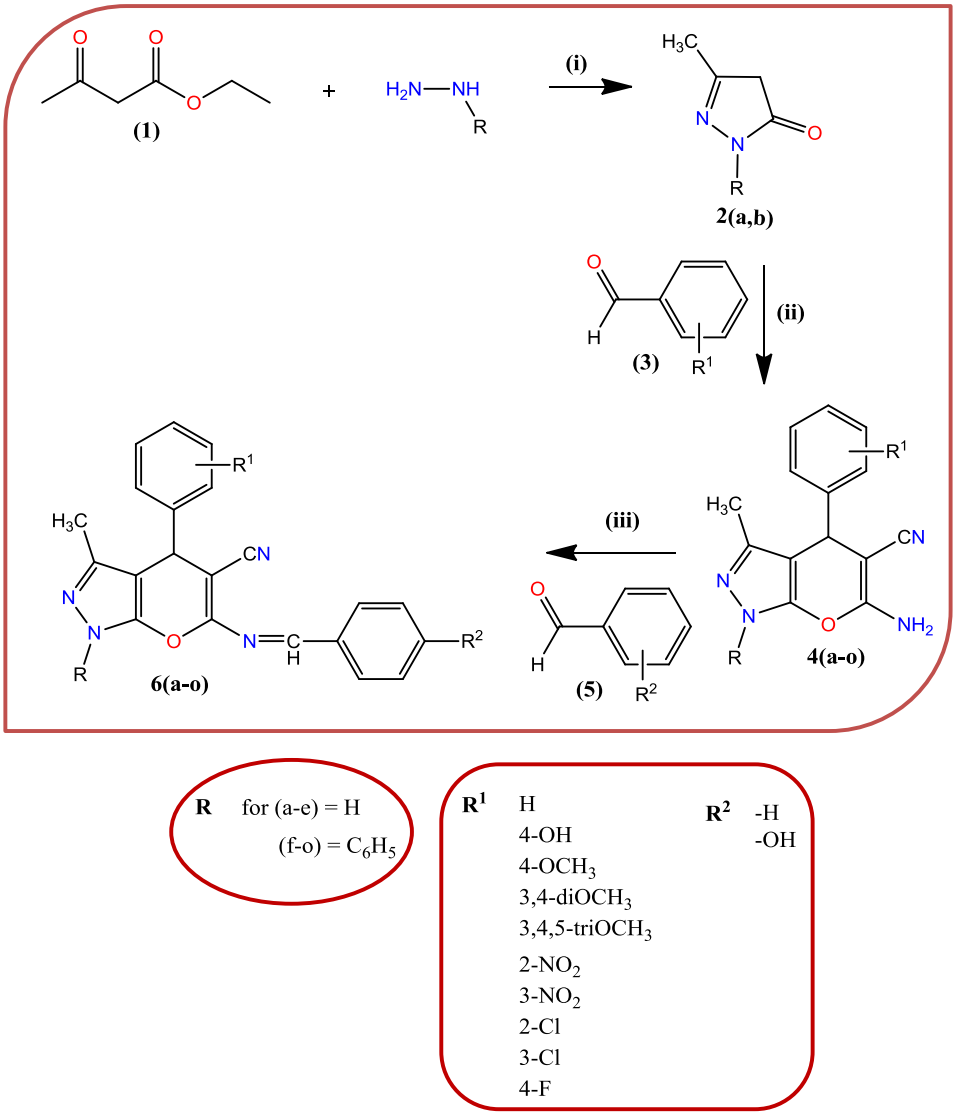

Scheme 1. Reagents & Conditions: (i) stirring at room temperature (ii) melononitrile, piperidine, 2 hr (iii) EtOH, AcOH, 3 h, Reflux.

reduced the anti-inflammatory activity. For the compounds substituted with electron-donating groups like methoxy and hydroxyl have weakened anti-inflammatory activity. The trimethoxy substitution (**6j**) diminished and mono substitution (**6h**) enhanced the *in vivo* activity. Looking at the effect of dimethoxy substitution, phenyl substituted pyrazole derivative (**6i**) has enriched and unsubstituted pyrazole derivative (**6b**) has greatly reduced anti-inflammatory activity. Similarly, unsubstituted compound at R^1 position of phenyl ring for compound **6f** displayed least activity stressing the significance of substitution.

2.6.3. Acute ulcerogenic studies

Based on the *in vivo* anti-inflammatory, compounds **6h, 6i, 6k, 6m** and **6o** were selected for the ulcerogenic screening. Aspirin and Ibuprofen were taken as standard drugs for the study. Results exhibited celecoxib with 1.204 ± 0.06 aspirin with 2.358 ± 0.28 and ibuprofen 2.1 ± 0.16 as Ulcer Index (Table 5). Comparatively all the five active compounds exhibited lesser ulcerogenic activity in the range of 0.603 ± 0.15 to 1.991 ± 0.34 and found to be safe. But one of the active compound **6o** demonstrated higher ulcerogenic activity with index of 1.991 ± 0.34. The other four compounds **6h**, **6i**, **6m** and **6k** showed ulecrogenic activity of 0.603, 0.642, 0.732 and 0.794 respectively with good GI safety profile. The most active compound **6k** with an ED_{50} of 0.8575 mmol/kg has shown ulcer index of 0.794 ± 0.09 which is almost 2.96 folds higher than aspirin and 2.64 folds higher and safer than ibuprofen.

2.6.4. In vitro cyclooxygenase (COX) inhibition studies

The COX-1 and COX-2 inhibition studies were carried out by Enzyme Immunoassay (EIA) method with the ovine COX-1 and the human recombinant COX-2. IC_{50} values i.e. the inhibitory concentration values were calculated and the experimental results is shown in the Table 5. Selectivity Index (SI) of compounds was determined by using the formula IC_{50} of COX-1/COX-2. The experiment was conducted as per the protocol described in the assay kit. Celecoxib, selective COX-2 inhibitor was screened as standard for both COX-1 and COX-2 inhibition and the study identified with SI of 147.05. All the tested compounds except **6c** and **6n** have exhibited COX-1 inhibition greater than 50 μM signifying that the design approach is selective to COX-2 inhibition. Compounds (**6a-o**) demonstrated selective COX-2 inhibition in the range of 2.560–38.12 μM except **6d**. The 2-chloro substituted compound **6d** was found least active with COX-2 inhibition of 108.12 μM. Comparison of experimental COX-2 inhibition in pIC_{50} with AutoQSAR predicted pIC_{50} values of compounds (**6a-o**) have shown satisfactory regression value of 0.7216 (Fig. 6). Further pharmacophore screening of chemical databases and prediction of COX-2 inhibition by QSAR model will identify potential molecules.

Table 3
Physical Characterization data of Pyrazole Derivatives.

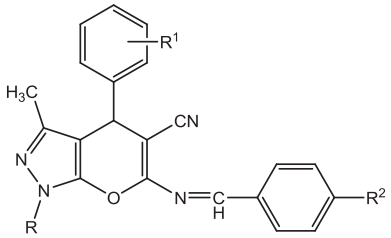

Compound Code	R	R^1	R^2	Molecular formula	Molecular weight	Melting point (^{0}C)	Yield %
6a	H	4-OH	OH	$C_{21}H_{16}N_4O_3$	372.38	175–177	30
6b	H	3,4-diOCH_3	H	$C_{23}H_{20}N_4O_3$	400.43	160–162	42
6c	H	2-NO_2	H	$C_{21}H_{15}N_5O_3$	385.38	210–212	35
6d	H	2-Cl	H	$C_{21}H_{15}ClN_4O$	374.82	180–182	30
6e	H	4-F	OH	$C_{21}H_{15}FN_4O_2$	374.37	185–187	45
6f	C_6H_5	H	H	$C_{27}H_{20}N_4O$	416.47	160–162	48
6g	C_6H_5	4-OH	H	$C_{27}H_{20}N_4O_2$	432.47	280–283	42
6h	C_6H_5	4-OCH_3	OH	$C_{28}H_{22}N_4O_3$	462.50	215–218	38
6i	C_6H_5	3,4-diOCH_3	H	$C_{29}H_{24}N_4O_3$	476.53	160–162	32
6j	C_6H_5	3,4,5-triOCH_3	OH	$C_{30}H_{26}N_4O_5$	522.55	225–227	40
6k	C_6H_5	2-NO_2	H	$C_{27}H_{19}N_5O_3$	461.57	210–212	42
6l	C_6H_5	3-NO_2	H	$C_{27}H_{19}N_5O_3$	461.57	145–147	44
6m	C_6H_5	2-Cl	H	$C_{27}H_{19}ClN_4O$	450.92	120–122	40
6n	C_6H_5	3-Cl	OH	$C_{27}H_{19}ClN_4O_2$	466.92	178–180	45
6o	C_6H_5	4-F	OH	$C_{27}H_{19}FN_4O_2$	450.46	206–208	46

Looking at the SAR of COX-2 inhibition, following compounds (**6a-o**) can be categorized into two series. The compounds were categorized as (**6a-e**) as one series and (**6f-o**) as another series with pyrazole ring unsubstituted and substituted with phenyl ring. The second series (**6f-o**) have exhibited potent and selective COX-2 inhibition highlighting the significance of phenyl ring substituted to nitrogen of pyrazole ring. Surprisingly, the least active compound **6d** with an IC_{50} value of 108.12 μM is among the series of (**6a-e**). Among the compounds, 3,4,5-trimethoxy derivative **6j** and 4-methoxy derivative **6h** were found with highest COX-2 inhibition at an IC_{50} of 2.56 and 4.32 μM. It can be noticed that substitution of methoxy group at 4th position is essential. Similarly, looking at the other compounds substituted with methoxy group **6b** and **6i** (3,4-dimethoxy) presented 6.24 and 11.48 μM. Substitution of chlorine at 3rd position for compound **6n** has demonstrated 7.75 μM and surprisingly substitution at 2nd position for **6m** has diminished the activity with 32.11 μM. Also substitution of fluoro group

Table 4
In vitro Human Red Blood Cell (HRBC) stability and In vivo anti-inflammatory activity of synthesized pyrazole derivatives in carrageenan induced paw edema model in rats.

Group	Treatment	R^1	% Membrane stability[a]	Edema volume at (Mean ± SEM)			
				1 h[b]	**2 h**[b]	**3 h**[b]	**4 h**[b]
1	**Toxicant control**[c]		—	1.18 ± 0.05	1.22 ± 0.05	1.27 ± 0.05$^{\#}$	1.40 ± 0.02$^{\#\#}$
2	**Ibuprofen**[d]		75.03 ± 0.013	0.96 ± 0.02*	1.00 ± 0.10	0.90 ± 0.04**	0.87 ± 0.01**
3	**Celecoxib**[d]		72.01 ± 0.010	0.90 ± 0.03*	0.94 ± 0.12	0.84 ± 0.04**	0.82 ± 0.02**
4	**6a**	4-OH	66.23 ± 0.024	1.25 ± 0.02	1.16 ± 0.02	1.00 ± 0.04*	0.96 ± 0.03**
5	**6b**	3,4-diOCH_3	59.92 ± 0.006	1.16 ± 0.06	1.13 ± 0.05	1.05 ± 0.05	0.99 ± 0.03**
6	**6c**	2-NO_2	70.14 ± 0.007	1.06 ± 0.05	1.05 ± 0.05	1.00 ± 0.03*	0.95 ± 0.03**
7	**6d**	2-Cl	69.94 ± 0.017	1.08 ± 0.08	1.06 ± 0.06	1.05 ± 0.03*	0.94 ± 0.04**
8	**6e**	4-F	71.14 ± 0.008	1.20 ± 0.04	1.20 ± 0.04	1.18 ± 0.05	0.98 ± 0.08**
9	**6f**	H	59.51 ± 0.019	1.10 ± 0.03	1.09 ± 0.08	1.00 ± 0.03*	1.00 ± 0.01**
10	**6g**	4-OH	64.36 ± 0.054	1.23 ± 0.06	1.12 ± 0.06	1.15 ± 0.06	0.99 ± 0.03**
11	**6h**	4-OCH_3	61.82 ± 0.010	1.07 ± 0.05	1.13 ± 0.09	1.05 ± 0.06	0.98 ± 0.04**
12	**6i**	3,4-diOCH_3	63.4 ± 0.007	1.16 ± 0.06	1.09 ± 0.08	1.00 ± 0.03*	0.97 ± 0.01**
13	**6j**	3,4,5-triOCH_3	64.16 ± 0.013	1.12 ± 0.05	1.30 ± 0.10	1.15 ± 0.05	1.10 ± 0.05**
14	**6k**	2-NO_2	65.35 ± 0.010	1.07 ± 0.05	1.15 ± 0.09	1.05 ± 0.06	0.93 ± 0.04**
15	**6l**	3-NO_2	55.16 ± 0.006455	1.16 ± 0.06	1.30 ± 0.10	1.05 ± 0.12	1.00 ± 0.02**
16	**6m**	2-Cl	67.63 ± 0.017	1.12 ± 0.05	1.13 ± 0.09	1.03 ± 0.05	0.94 ± 0.04**
17	**6n**	3-Cl	56.15 ± 0.017	1.15 ± 0.09	1.11 ± 0.09	1.03 ± 0.06*	0.99 ± 0.05**
18	**6o**	4-F	71.18 ± 0.029	1.21 ± 0.05	1.15 ± 0.03	1.05 ± 0.05	0.95 ± 0.03**

Data are expressed as the mean ± SEM (n = 6/group) by using Student's *t*-test (significant at $p < 0.05$* and 0.01**) for carrageenan induced paw edema results and % membrane stability by using ordinary one way ANOVA (significant at $p < 0.0001$). The statistical significance of difference of carrageenan-control compared to vehicle-control group was shown as #$p < 0.05$, the statistical significance of difference in synthesized compounds and standard drugs (Ibuprofen and Celecoxib) treated groups as compared to carrageenan-control was designated as *$p < 0.01$. Values of edema volume without symbols like * and # were ns (non-significant).

[a] Values were presented as mean ± SEM (n = 6)

[b] Synthesized compounds were administered at dose of 200 mg/kg.

[c] Carrageenan was used at dose 0.1 ml (1% w/v).

[d] Standard drug Ibuprofen and Celecoxib was administered at dose of 40 mg/kg.

Table 5
In vitro COX-1 and COX-2 inhibition for pyrazoles (**6a-o**) and ulcerogenic activity.

Compound Code	COX-2 (IC_{50} in μM)	COX-2 pIC_{50}	Predicted pIC_{50}[a]	COX-1 (IC_{50} in μM)	COX-1 pIC_{50}	SI[b]	Ulcerogenic activity[c]
6a	11.71	4.931	5.4088	70.61	4.1511	6.029	ND[d]
6b	6.240	5.204	5.4694	100.78	3.9966	16.15	ND
6c	25.31	4.596	4.7738	37.72	4.4234	1.49	ND
6d	108.12	3.966	4.5940	282.77	3.5485	2.615	ND
6e	7.630	5.117	5.4088	51.32	4.2897	6.726	ND
6f	22.56	4.646	4.7248	112.63	3.9483	4.992	ND
6g	7.220	5.141	5.4405	87.72	4.0569	12.14	ND
6h	4.320	5.364	5.2796	276.44	3.5583	63.99	0.603 ± 0.15
6i	11.48	4.940	5.5909	300.72	3.5218	26.19	0.642 ± 0.25
6j	2.560	5.591	6.2462	82.22	4.0850	32.11	ND
6k	38.12	4.418	4.9055	208.76	3.6803	5.476	0.794 ± 0.09
6l	25.87	4.587	4.9055	76.67	4.1153	2.963	ND
6m	32.11	4.493	4.7248	301.42	3.5208	9.387	0.732 ± 0.18
6n	7.750	5.110	5.4405	33.58	4.4739	4.332	ND
6o	21.87	4.660	5.4405	225.68	3.6465	10.31	1.991 ± 0.34
Ibuprofen	ND	ND	ND	ND	ND	ND	2.100 ± 0.16
Celecoxib	0.34	6.468	ND	> 50.00	> 4.301	147.05	1.204 ± 0.06
Aspirin	ND	ND	ND	ND	ND	ND	2.358 ± 0.28

[a] COX-2 Inhibition values predicted from AutoQSAR model
[b] Selectivity Index of compounds IC_{50} of COX-1/IC_{50} of COX-2
[c] Values represents the Severity Index ± S.E.M
[d] ND- Not Determined

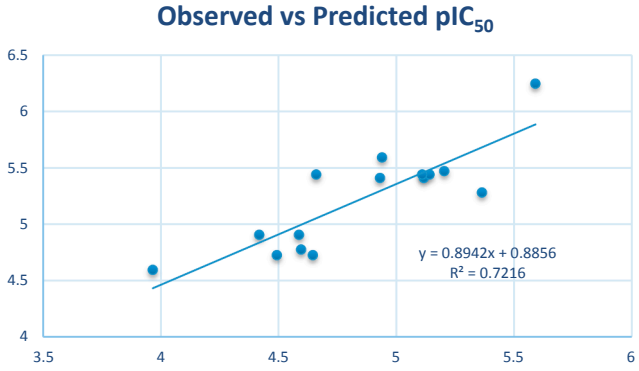

Fig. 6. Plot of COX-2 Inhibition pIC_{50} (experimental) vs AutoQSAR pIC_{50} (predicted) for synthesized pyrazole derivatives.

at 4th position for **6o** has reduced with 21.87 μM. Substitution of nitro group at 2nd and 3rd position for **6k**, **6l** has showed 38.12 and 25.87 μM respectively. In the series of (**6a-e**), compounds **6b**, **6e** and **6a** have exhibited good COX-2 inhibition with an IC_{50} values of 6.24, 7.63 and 11.71 μM respectively. With respect to Selectivity Index (SI), compound **6h** has shown higher value of 63.99, among all the synthesized compounds. The compounds **6i** and **6j** were observed with 26.19 and 32.11. Similarly compounds **6b**, **6m** and **6o** were found moderately selective with 16.15, 9.387 and 10.31 respectively. Except **6d**, all the compounds exhibited moderate to potent and selective COX-2 inhibition profile. The overall results suggests that substitution of phenyl group to nitrogen of pyrazole and methoxy group at 3rd and 4th position, chloro group at 3rd position of R^2 are crucial for potent and selective COX-2 inhibition.

2.7. Pharmacophore hypothesis screening of synthesized pyrazole derivatives and correlation with experimental results

Synthesized pyrazole derivatives were screened through ligand based pharmacophore model to investigate the specificity towards COX-2 enzyme. Interestingly all the 15 compounds passed through the nominated and validated hypothesis. The AHHR_1 suggests that compounds exhibited anti-inflammatory activity by inhibition of COX-2 enzyme. Compounds have displayed fitness score for the hypothesis in the range of 1.104–1.671 except one compound **6n** with a score of 0.551 (Table 6). But the fitness score of standard drugs i.e., selective COX-2 inhibitors was observed in the range of 1.265–2.558 indicating that compounds were less or moderately active inhibitors.

Table 6
Correlation of *in vivo* anti-inflammatory, *in vitro* COX-2 Inhibition values and hypothesis screening scores of synthesized pyrazole derivatives.

Code	ED_{50}[a]		Matched ligand sites	Fitness score	Vector score	Volume score	pIC50 (obs.)
	mg/kg	mmol/kg					
6a	436.5	1.1721	3	1.585	0.889	0.402	4.931
6b	483.1	1.2064	4	1.155	0.839	0.380	5.204
6c	422.5	1.0963	3	1.601	0.889	0.419	4.596
6d	417.3	1.1133	3	1.602	0.889	0.419	3.966
6e	466.7	1.2466	3	1.671	0.935	0.359	5.117
6f	499.8	1.2000	3	1.662	0.889	0.480	4.646
6g	483.1	1.1170	3	1.651	0.889	0.469	5.141
6h	466.7	1.0090	4	1.106	0.839	0.332	5.364
6i	451.3	0.9470	4	1.119	0.839	0.344	4.940
6j	733.7	1.4040	4	1.104	0.839	0.329	5.591
6k	395.8	0.8575	3	1.63	0.889	0.448	4.418
6l	499.8	1.0828	3	1.61	0.889	0.427	4.587
6m	417.3	0.9254	3	1.642	0.889	0.459	4.493
6n	483.1	1.0346	4	0.551	0.628	0.332	5.110
6o	422.5	0.9379	3	1.641	0.889	0.459	4.660
Ibuprofen	4.606	22.359	ND	ND	ND	ND	ND
Celecoxib	3.060	8.0314	ND	ND	ND	ND	ND

[a] ED_{50} was calculated for 200 mg/kg of compounds after 4 h.

To further investigate, *in vitro* COX-2 inhibition pIC_{50} values of synthesized pyrazole derivatives were correlated with fitness score of hypothesis. The COX-2 inhibition pIC_{50} values of compounds **6(a-o)** were observed in the range of 3.966–5.591. All the values were depicted in Table 5. The present hypothesis could filter all the compounds as selective COX-2 inhibitors and experimental COX-2 inhibition values too support the same. But poor correlation was observed between fitness score and experimental pIC_{50} values. However, compound **6n** was observed with highest COX-1 inhibition of 33.58 μM and was found with least fitness score of 0.551. The Pharmacophore hypothesis screening, being a qualitative approach helps in identifying the lead for selective COX-2 inhibition and was validated with marketed anti-inflammatory drugs.

For the comparison of experimental *in vitro* and *in vivo* results with

in silico data, five compounds **6k**, **6m**, **6o**, **6i** and **6h** have exhibited *in vivo* anti-inflammatory activity below 1 mmol/kg. The human RBC membrane stabilizing property of these compounds was observed in the range of 61.83–71.2. Overall range observed for the compounds (**6a-o**) was 55.15 to 71.2 and it appears quite impressive in terms of correlation. Similarly, observed COX-2 inhibition values in pIC_{50} was in a range of 3.966–5.591. The overall results of *in vitro* and *in vivo* anti-inflammatory activities reveals that design approach is selective to COX-2 inhibition and active molecules are safer than standard NSAIDs in the market. Surprisingly, the compounds like **6j** and **6h** have shown potential *in vitro* COX-2 inhibition but failed to show *in vivo* anti-inflammatory activity. But the compounds **6k** and **6m** exhibited good *in vivo* anti-inflammatory activity but poor *in vitro* COX-2 inhibition. However the *in vivo* active compounds were found with lesser ulcerogenic activity related to standard drugs in the market. Extending the *in vivo* study for few more hours or conducting the pharmacokinetic study of active compounds might help in better understanding the SAR and correlation of *in vitro* vs *in vivo* activity. Also further modifications in the structure might produce a potent and safer molecule from this series.

3. Conclusion

Compounds substituted with electron-withdrawing group nitro and halogens like chloro, fluoro at ortho position indicated a significant anti-inflammatory activity while the same substitution at meta position showed a moderate activity. From the design aspects, structural features with experimental therapeutic and toxicity evaluation, further structural modifications of identified lead molecule might benefit a potent COX-2 inhibitor from this series. Pharmacophore model can be exploited for the screening chemical databases of both natural and synthetic compounds for lead identification and repositioning of drugs. With the SAR findings and further structural modifications of lead molecule with assistance of selected QSAR model can serve in the design of potent, selective and safe COX-2 inhibitor in future.

4. Experimental section

4.1. Dataset for pharmacophore and QSAR modelling

The chemical structures of 37 substituted pyrazoles as selective COX-2 inhibitors were collected from the literature as shown in Table 7a-7d [29,30]. From the series, 25 compounds were taken as one set to build pharmacophore and QSAR modelling and remaining 12 compounds were used to validate the models. All the compounds were synthesized, characterized, screened for both COX-1 & COX-2 inhibition assay and *in vivo* anti-inflammatory study by same method. Chemical structures of compounds were sketched using Meastro 3D Builder and energy minimization was performed using Ligprep module[31]. To

Table 7b
Chemical structures of substituted pyrazoles (Group II).

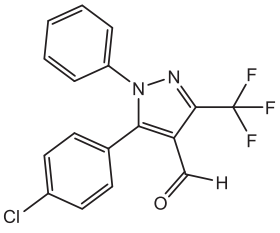

1.5

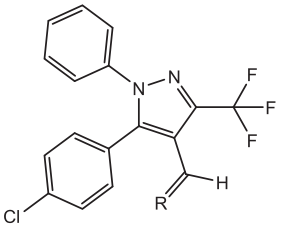

1.6a-1.6f

Compound Code	R	Compound Code	R
1.6a	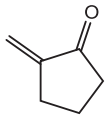	1.6d	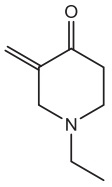
1.6b	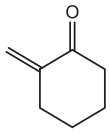	1.6e	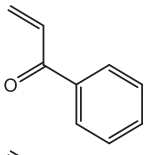
1.6c	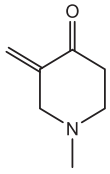	1.6f	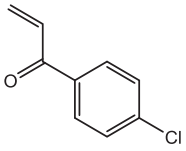

Table 7a
Chemical structures of substituted pyrazoles (Group I).

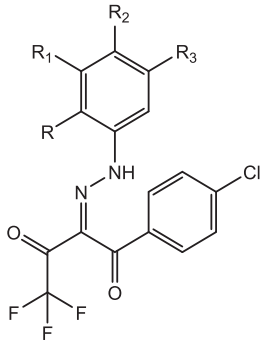

1.2a-1.2f

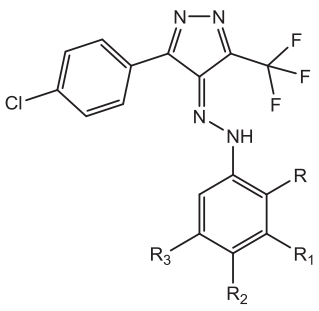

1.3a-1.3f

Compound Code		R	R_1	R_2	R_3
1.2a	1.3a	Cl	H	H	H
1.2b	1.3b	H	H	Cl	H
1.3c	1.3c	H	H	Br	H
1.2d	1.3d	H	H	NO_2	H
1.2e	1.3e	H	H	OCH_3	H
1.2f	1.3f	H	CF_3	H	CF_3

Table 7c
Chemical structures of substituted pyrazoles (Group III).

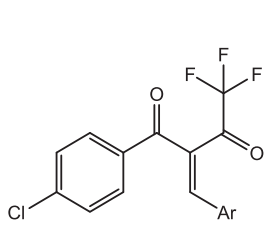

2.2a-2.2f

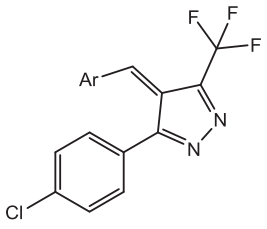

2.3a-2.3f

Compound Code		Ar	Compound Code		Ar
2.2a	2.3a	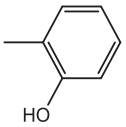	2.2d	2.3d	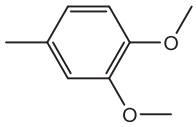
2.2b	2.3b	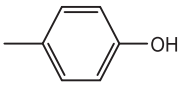	2.2e	2.3e	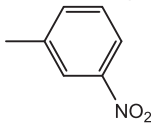
2.2c	2.3c	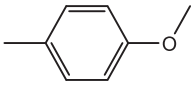	2.2f	2.3f	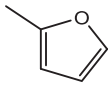

Table 7d
Chemical structures of substituted pyrazoles (Group IV).

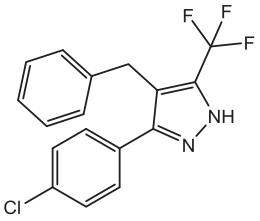

2.5

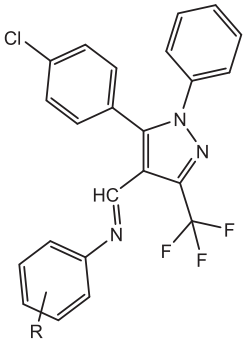

2.8a-2.8d

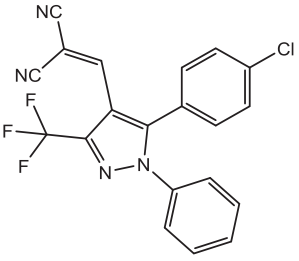

2.9

Compound Code	R	Compound Code	R
2.8a	4-Br	2.8c	4-NO_2
2.8b	2-Cl	2.8d	3,5-diCF_3

simplify the input data for *in silico* computational studies, IC_{50} values of all the compounds were converted to pIC_{50}. The dataset of 25 compounds were randomly divided to training and test sets in the ratio of 80:20 for building QSAR using an advanced tool of Schrodinger Drug Design Suite [32], AutoQSAR.

4.2. Building and validation of pharmacophore model

The ligand based pharmacophore models were built for selected 25 pyrazole derivatives from the published literature and all the synthesized pyrazoles were biologically tested for both COX-1 & COX-2 inhibition and *in vivo* anti-inflammatory activity. Chemical structures of the compounds were sketched with Maestro 3D Builder [33]. IC_{50} values of all the compounds were added as separate column and computed to logarithmic values (pIC_{50}) in the project table of Maestro. Pharmacophore model was built with an option of creating hypothesis with multiple ligands using Phase module of Schrodinger Drug Design Suite [34]. Study was continued with default options like generate and minimize 50 conformers for each molecule, generated hypothesis should match atleast 50% of all the actives and preferred up to 5 features with a minimum of 4 features in each hypothesis. It was allowed to generate and display top 10 models based on Phase HypoScore. Hypothesis generated will have features in combination of hydrogen bond acceptor (A), hydrogen bond donor (D), hydrophobic (H), negative (N), positive (P) and aromatic rings (R). The top hypothesis was selected based on the scoring parameters and validated with a set of 12 molecules screened by same biological assay method and standard drugs to evaluate the selectivity of COX-1 and COX-2 inhibitors. All the molecules were aligned to selected model and calculated fitness, vector and volume scores. After validation of selected pharmacophore, synthesized pyrazole derivatives were screened to calculate the scores and to investigate the molecular features required for COX-2 inhibition. The model was evaluated for sensitivity and specificity with small dataset of molecules and drugs using below formulae [35].

$$\text{Sensitivity} = \frac{\text{found actives}}{\text{all actives in database}}$$

$$\text{Specificity} = \frac{\text{found inactives}}{\text{all inactives in database}}$$

4.3. Building an AutoQSAR model

QSAR model was built for the same 25 substituted pyrazoles used for building Pharmacophore model by an advanced and automated tool AutoQSAR [36]. It is an advanced and automated tool which correlates around 497 physicochemical topological properties to quantify the structural features and therapeutic inhibition. For the study, pyrazole derivatives were categorized randomly to 80:20 ratio of training and test sets. The tool randomly filters loaded molecules into training and test set and screens through the statistical algorithms like multiple linear regression (MLR), partial least square regression (PLS), kernel based PLS (KPLS), principal component regression (PCR), etc and ranks the models based on R^2, $Q^2$and standard deviation values. Best QSAR model was selected i.e., kpls_molprint2D_45 and used for prediction of COX-2 inhibition values.

4.4. Chemistry

All the chemicals and solvents were purchased from suppliers such as Sigma-Aldrich, Merck, Fisher Scientific etc., and utilized as received. All the reactions were carried out in anhydrous conditions under nitrogen gas. Readymade pre-coated silica gel 60 F_{254}-coated thin-layer chromatography (TLC) plates from Merck Chemicals (Whitehouse Station, NJ), and were visualized with UV light and Iodine chamber. Final compounds were purified by Column Chromatography packed with silica gel Merck Grade 60 (230–400 mesh, 60 Å). Melting points of compounds were recorded on a Tempirol hot-stage with microscope and are uncorrected. UV spectra were recorded in MeOH on a Shimadzu-UV-1601 spectrophotometer; ^{1}H- and ^{13}C NMR spectra were taken in DMSO-d_6 solution in a 5-mm tube on a Bruker drx 500 Fourier transform spectrometer with tetramethylsilane as internal standard. Molecular weight information was obtained from ESI mass spectrometry (Supplementary Information).

4.4.1. Synthesis of 3-methyl-pyrazole-5-one (2a) [37]:

To a solution of ethylacetoacetate (1.3 ml, 0.01 mol) (1) was added hydrazine hydrate (0.5 ml, 0.01 mol) drop wise with constant stirring at room temperature. Precipitate formed quickly, as the reaction was exothermic and was permitted to cool at room temperature. The crude product separated was filtered and recrystallized using absolute ethanol gave 70% yield: mp 222–224 ^{0}C.^{1}HNMR (DMSO-d_6): δ 10.3–10.4 (s, 2H, OH and NH); 5.2–5.3 (s, 1H, −CH =); 2.0–2.1 (s, 3H, $-CH_3$). ^{13}CNMR (DMSO-d_6): δ173.62, 159.54, 45.17, 16.42. MS (*m/z*): 99.21 [M + 1]; IR (KBr) cm^{-1}: 1800 (C═O)

4.4.2. Synthesis of 3-methyl-1-phenylpyrazole-5-one (2b)[37]

To a solution of ethylacetoacetate (1.3 ml, 0.01 mol) (1) was added phenyl hydrazine (1.8 ml, 0.01 mol) drop wise with constant stirring. The mixture was allowed to heat on boiling water bath in fuming hood for about 2 h with constant stirring. Allowed till heavy reddish syrup to cool at room temperature, added 25 ml of ether and stirring was continued. The insoluble syrup in ether was solidified within 15 min. The crude solid separated was filtered and washed with excess ether to remove the colored and other impurities. The product was recrystallized from hot water giving 70% yield:mp 125–127 ^{0}C.^{1}HNMR (DMSO-d_6) δ: 7.1–7.9 (m, 5H, Ar-H); 3.4–3.5 (s, 2H, $-CH_2$); 2.0–2.1 (s, 3H, $-CH_3$). ^{13}CNMR (DMSO-d_6) δ: 176.51, 162.84, 138.95, 124.62, 125.21, 128.97, 126.24, 128.05, 42.56, 16.72. MS (*m/z*): 175.35 [M + 1]. IR (KBr) cm^{-1}: 1800 (C═O), 3030 (−CH).

4.4.3. Synthesis of 6-amino-3-methyl-1-substituted-4-phenyl-1,4-dihydropyrano[2,3-c]pyrazol-5-carbonitriles (4a-o)

To the mixture of melanonitrile (0.6 ml, 0.01 mol) and substituted aromatic aldehydes (0.01 mol) in absolute ethanol (15 ml), appropriate 2a or 2b (0.01 mol) was added with constant stirring. After the slow addition of piperidine (0.5 ml) stirring was continued for 2 h. Progress of reaction was further monitored by TLC for completion and the solvent was vaporized under vacuum to dryness.

4.4.3.1. 6-amino-4-(4-hydroxyphenyl)-3-methyl-1,4-dihydropyrano[2,3-c]pyrazole-5-carbonitrile (4a). The crude product was recrystallized from absolute ethanol giving 60% yield mp 210–212 ^{0}C.^{1}HNMR (DMSO-d_6) δ: 10.8–11.2 (s, 1H, NH), 6.5–7.2 (m, 4H, Ar-H), 5.6–5.7 (d, 1H, pyran), 4.7–4.9 (d, 2H, NH_2), 3.8–3.9 (s, 1H, OH), 1.8–2.0 (s, 3H, CH_3).MS (*m/z*): 269.14 [M + 1]. IR (KBr) cm^{-1}: 3650, 3287 (−NH and $-NH_2$); 2815 (Ar-CH).

4.4.3.2. 6-amino-4-(3,4-methoxyphenyl)-3-methyl-1,4-dihydropyrano[2,3-c]pyrazole-5-carbonitrile (4b). The crude product was recrystallized from absolute ethanol giving 68% yield mp 188–190 ^{0}C.^{1}HNMR (DMSO-d_6) δ: 9.8–10.2 (s, 1H, NH), 6.7–7.5 (m, 3H, Ar-H), 5.2–5.5 (d, 1H, pyran), 4.6–4.8 (d, 2H, NH_2), 3.8–3.9 [d, 6H, $(OCH_3)_2$], 1.8–1.9 (s, 3H, CH_3).MS (*m/z*): 312.54 [M +]. IR (KBr) cm^{-1}: 2180 (−CN), 3030, 3560 (−NH and $-NH_2$); 2835 (Ar-CH).

4.4.3.3. 6-amino-4-(2-nitrophenyl)-3-methyl-1,4-dihydropyrano[2,3-c]pyrazole-5-carbonitrile (4c). The crude product was recrystallized from absolute ethanol giving 72% yield mp 230–232 ^{0}C.^{1}HNMR (DMSO-d_6) δ: 10.6–11.3 (s, 1H, NH), 7.8–8.8 (m, 4H, Ar-H), 5.5–5.6 (d, 1H, pyran), 4.9–5.2 (d, 2H, NH_2), 1.4–1.9 (s, 3H, CH_3).MS (*m/z*): 298.71 [M + 1]. IR (KBr) cm^{-1}: 2220 (−CN), 3400, 3580 (−NH and $-NH_2$); 2714 (Ar-CH).

4.4.3.4. 6-amino-4-(2-chlorophenyl)-3-methyl-1,4-dihydropyrano[2,3-c]pyrazole-5-carbonitrile (4d). The crude product was recrystallized from absolute ethanol giving 64% yield mp 240–242 ^{0}C.^{1}HNMR (DMSO-d_6) δ: 10.8–11.2 (s, 1H, NH), 7.2–8.2 (m, 4H, Ar-H), 5.6–5.7 (d, 1H, pyran), 4.9–5.1 (d, 2H, NH_2), 2.0–2.2 (s, 3H, CH_3).MS (*m/z*): 288.56 [M + 1]. IR (KBr) cm^{-1}: 2191 (−CN), 3630, 3387 (−NH and $-NH_2$); 2924 (Ar-CH).

4.4.3.5. 4.4.3.5. 6-amino-4-(2-fluorophenyl)-3-methyl-1,4-dihydropyrano[2,3-c]pyrazole-5-carbonitrile (4e). The crude product was recrystallized from absolute ethanol giving 75% yield mp 230–232 ^{0}C.^{1}HNMR (DMSO-d_6) δ: 11.3–11.9 (s, 1H, NH), 7.2–8.2 (m, 4H, Ar-H), 5.6–5.8 (d, 1H, pyran), 5.2–5.5 (d, 2H, NH_2), 2.0–2.3 (s, 3H, CH_3).MS (*m/z*): 271.34 [M + 1]. IR (KBr) cm^{-1}: 2191 (−CN), 3500, 3387 (−NH and $-NH_2$); 2824 (Ar-CH).

4.4.3.6. 6-amino-3-methyl-1,4-diphenyl-1,4-dihydropyrano[2,3-c]pyrazole-5-carbonitrile (4f). The crude product was recrystallized from absolute ethanol giving 65% yield mp 140–142 ^{0}C.^{1}HNMR (DMSO-d_6) δ: 6.6–7.5 (m, 10H, Ar-H), 4.2–4.3 (d, 1H, pyran), 4.8–5.1 (d, 2H, NH_2), 2.0–2.2 (s, 3H, CH_3).MS (*m/z*): 329.57 [M + 1]. IR (KBr) cm^{-1}: 2160 (−CN), 3333 (−NH); 2900, 2840 (Ar-CH).

4.4.3.7. 6-amino-4-(4-hydroxyphenyl)-3-methyl-1-phenyl-1,4-dihydropyrano[2,3-c]pyrazole-5-carbonitrile (4 g). The crude product was recrystallized from absolute ethanol giving 67% yield mp 194–196 ^{0}C.^{1}HNMR (DMSO-d_6) δ: 6.5–7.2 (m, 9H, Ar-H), 5.6–5.7 (d, 1H, pyran), 4.7–4.9 (d, 2H, NH_2), 3.8–3.9 (s, 1H, OH), 1.8–2.0 (s, 3H, CH_3).MS (*m/z*): 345.36 [M + 1]. IR (KBr) cm^{-1}: 2194 (−CN), 3260 (−NH); 2980, 2838 (Ar-CH).

4.4.3.8. 6-amino-4-(4-methoxyphenyl)-3-methyl-1-phenyl-1,4-dihydropyrano[2,3-c]pyrazole-5-carbonitrile (4 h). The crude product was recrystallized from absolute ethanol giving 70% yield mp 170–174 ^{0}C.^{1}HNMR (DMSO-d_6) δ: 6.7–7.7 (m, 9H, Ar-H), 5.8–5.9 (d,

1H, pyran), 3.8–3.9 [d, 3H, OCH_3], 4.7–4.9 (d, 2H, NH_2), 1.9–2.0 (s, 3H, CH_3).MS (*m/z*): 359.82 [M + 1]. IR (KBr) cm^{-1}: 2150 (−CN), 3370 (−NH); 2970, 2854 (Ar-CH).

4.4.3.9. 6-amino-4-(3,4-dimethoxyphenyl)-3-methyl-1-phenyl-1,4-dihydropyrano[2,3-c]pyrazole-5-carbonitrile (4i). The crude product was recrystallized from absolute ethanol giving 78% yield mp 130–132 ^{0}C.^{1}HNMR (DMSO-d_6) δ: 6.7–7.7 (m, 8H, Ar-H), 4.7–4.8 (d, 2H, NH_2),4.6–5.2 (d, 1H, pyran), 3.8–3.9 [d, 6H, $(OCH_3)_2$], 1.9–2.0 (s, 3H, CH_3).MS (*m/z*): 387.22 [M − 1]. IR (KBr) cm^{-1}: 2193 (−CN), 3300 (−NH_2); 2835 (Ar-CH).

4.4.3.10. 6-amino-4-(3,4,5-trimethoxyphenyl)-3-methyl-1-phenyl-1,4-dihydropyrano[2,3-c]pyrazole-5-carbonitrile (4j). The crude product was recrystallized from absolute ethanol giving 65% yield mp 160–162 ^{0}C.^{1}HNMR (DMSO-d_6) δ: 6.7–7.7 (m, 7H, Ar-H), 5.8–5.9 (d, 1H, pyran), 4.7–4.9 (d, 2H, NH_2), 3.8–3.9 [d, 9H, $(OCH_3)_3$], 1.9–2.0 (s, 3H, CH_3).MS (*m/z*): 419.71 [M + 1].IR (KBr) cm^{-1}: 2178 (−CN), 3300 (−NH_2); 2910, 2800 (Ar-CH).

4.4.3.11. 6-amino-4-(2-nitrophenyl)-3-methyl-1-phenyl-1,4-dihydropyrano[2,3-c]pyrazole-5- carbonitrile (4 k). The crude product was recrystallized from absolute ethanol giving 66% yield mp 135–137 ^{0}C.^{1}HNMR (DMSO-d_6) δ: 7.1–8.1 (m, 9H, Ar-H), 4.0–5.0 (d, 2H, NH_2), 5.2–5.4 (d, 1H, pyran), 1.8–1.9 (s, 3H, CH_3).MS (*m/z*): 373.25 [M +]. IR (KBr) cm^{-1}: 2198 (−CN), 3180 (−NH_2); 2990, 2740 (Ar-CH).

4.4.3.12. 6-amino-4-(3-nitrophenyl)-3-methyl-1-phenyl-1,4-dihydropyrano[2,3-c]pyrazole-5-carbonitrile (4 l). The crude product was recrystallized with absolute ethanol giving 78% yield mp 188–190 ^{0}C.^{1}HNMR (DMSO-d_6) δ: 7.6–8.6 (m, 9H, Ar-H), 4.9–5.2 (d, 2H, NH_2), 5.5–5.6 (d, 1H, pyran), 1.2–1.6 (s, 3H, CH_3).MS (*m/z*): 373.36 [M +]. IR (KBr) cm^{-1}: 2170 (−CN), 3150 (−NH_2); 2920, 2730 (Ar-CH).

4.4.3.13. 6-amino-4-(2-chlorophenyl)-3-methyl-1-phenyl-1,4-dihydropyrano[2,3-c]pyrazole-5-carbonitrile (4 m). The crude product was recrystallized from absolute ethanol giving 77% yield mp 142–145 ^{0}C; ^{1}HNMR (DMSO-d_6) δ: 7.1–8.2 (m, 9H, Ar-H), 4.9–5.1 (d, 2H, NH_2), 5.6–5.8 (d, 1H, pyran), 2.0–2.2 (s, 3H, CH_3).MS (*m/z*): 364.81 [M + 1]. IR (KBr) cm^{-1}: 2196 (−CN), 3387 (−NH_2); 2918, 2837 (Ar-CH).

4.4.3.14. 6-amino-4-(3-chlorophenyl)-3-methyl-1-phenyl-1,4-dihydropyrano[2,3-c]pyrazole-5-carbonitrile (4n). The crude product was recrystallized from absolute ethanol giving 69% yield mp 160–162 ^{0}C.^{1}HNMR (DMSO-d_6) δ: 7.4–7.9 (m, 9H, Ar-H), 4.6–5.2 (d, 2H, NH_2), 5.5–5.8 (d, 1H, pyran), 2.0–2.2 (s, 3H, CH_3).MS (*m/z*): 364.55 [M + 1]. IR (KBr) cm^{-1}: 2118 (−CN), 3340 (−NH_2); 2933, 2870 (Ar-CH).

4.4.3.15. 6-amino-4-(4-fluorophenyl)-3-methyl-1-phenyl-1,4-dihydropyrano[2,3-c]pyrazole-5-carbonitrile (4o). The crude product was recrystallized from absolute ethanol giving 70% yield mp 168–170 °C.^{1}HNMR (DMSO-d_6) δ: 7.8–8.8 (m, 9H, Ar-H), 5.2–5.5 (d, 2H, NH_2), 5.6–5.8 (d, 1H, pyran), 1.7–1.9 (s, 3H, CH_3).MS (*m/z*): 347.18 [M + 1]. IR (KBr) cm^{-1}: 2145 (−CN), 3374 (−NH_2); 2918, 2835 (Ar-CH).

4.4.4. Synthesis of 3-methyl-1-substituted-4-phenyl-6-[{(1E)-phenylmethylene}amino]1,4-dihyro pyrano[2,3-c] pyrazole-5-carbonitrile (6a-o)

A stirred solution of appropriated intermediates (4a-o, 0.004 mol) in absolute ethanol (25 ml) treated with substituted aldehydes (0.004 mol) in the presence of acetic acid (glacial, 1.0 ml) as catalyst and refluxed for 3 h. Then the reaction mixture was permitted to cool 0 ^{0}C and poured on to the crushed ice with vigorous stirring. The crude product separated was filtered, dried and purified by column chromatography with neutral alumina.

4.4.4.1. 4-(4-hydroxyphenyl)-3-methyl-6-[{(1E)-(4-hydroxyphenyl) methylene}amino]-1,4-dihydropyrano[2,3-c]pyrazole-5-carbonitrile (6a). The crude product was purified by eluting with mobile phase Hexane and AcOEt (75:25) affording 30% yield mp175-177 ^{0}C.^{1}HNMR (DMSO-d_6) δ: , 8.6–8.7 (s, 1H, CH = N), 7.8–7.9 (s, 1H, −OH), 6.9–7.9 (m, 8H, Ar-H), 4.2–4.6 (d, 1H, pyran), 2.1–2.4 (s, 3H, CH_3). ^{13}CNMR (DMSO-d_6) δ: 171.51, 163.74, 160.82, 155.87, 155.61, 131.84, 130.67, 130.62, 126.31, 129.54, 129.50, 117.31, 116.08, 116.04, 116.01, 116.00, 76.51, 71.23, 49.50, 26.57, 19.81. MS (*m/z*): 373.15 [M + 1]. IR (KBr) cm^{-1}: 2140 (−CN), 2916, 2815 (Ar-CH), 3204 (−OH).Anal. Calcd. For $C_{21}H_{16}N_4O_3$: C, 67.73; H, 4.33; N, 15.05;O, 12.89. Found C, 67.63; H, 4.29; N, 15.09; O, 12.85.

4.4.4.2. 4-(3,4-dimethoxyphenyl)-3-methyl-6-[{(1E)-phenylmethylene} amino]-1,4-dihydropyrano [2,3-c]pyrazole-5-carbonitrile (6b). The crude product was purified by eluting with mobile phase Hexane and AcOEt (70:30) affording 42% yield mp 160–162 ^{0}C; ^{1}HNMR (DMSO-d_6) δ: 8.6–8.7 (s, 1H, CH = N), 6.5–7.8 (m, 8H, Ar-H), 4.2–4.3 (d, 1H, pyran), 3.7–4.0 [d, 6H, $(OCH_3)_2$], 2.3–2.4 (s, 3H, CH_3). ^{13}CNMR (DMSO-d_6) δ: 171.52, 163.71, 155.66, 149.92, 147.13, 133.77, 132.59, 131.03, 129.25, 129.22, 128.86, 128.83, 121.41, 117.38, 112.52, 109.81, 76.50, 71.24, 56.17, 56.13, 49.52, 26.61, 20.18.MS (*m/z*): 401.35 [M + 1]. IR (KBr) cm^{-1}: 2160 (−CN), 2900, 2875 (Ar-CH).Anal. Calcd. For $C_{23}H_{20}N_4O_3$: C, 67.73; H, 4.33; N, 15.05; O, 12.89. Found C, 67.70; H, 4.28; N, 15.07; O, 12.86.

4.4.4.3. 4-(2-nitrophenyl)-3-methyl-6-[{(1E)-phenylmethylene}amino]-1,4-dihydropyrano[2,3-c]pyrazole-5-carbonitrile (6c). The crude product was purified by eluting with mobile phase Hexane and AcOEt (70:30) affording 35% yield mp 210–212 ^{0}C.^{1}HNMR (DMSO-d_6) δ: 8.2–8.4 (s, 1H, CH = N), 7.1–7.9 (m, 9H, Ar-H), 4.4–4.6 (d, 1H, pyran), 1.8–2.0 (s, 3H, CH_3). ^{13}CNMR (DMSO-d_6) δ: 165.62, 163.34, 152.57, 136.46, 136.22, 134.51, 131.08, 129.27, 129.23, 128.88, 128.86, 126.85, 126.14, 124.66, 122.71, 49.05, 42.71, 39.54, 28.89, 26.54, 14.82. MS (*m/z*): 386.27 [M + 1]. IR (KBr) cm^{-1}: 2170 (−CN), 2950, 2845 (Ar-CH).Anal. Calcd. For $C_{21}H_{15}N_5O_3$: C, 65.45; H, 3.92; N, 18.17; O, 12.46. Found C, 65.42; H, 3.89; N, 18.15; O, 12.42.

4.4.4.4. 4-(2-chlorophenyl)-3-methyl-6-[{(1E)-phenylmethylene}amino]-1,4-dihydropyrano [2,3-c]pyrazole-5-carbonitrile (6d). The crude product was purified by eluting with mobile phase Hexane and AcOEt (70:30) affording 30% yield mp 180–182 ^{0}C.^{1}HNMR (DMSO-d_6) δ: 8.8–8.9 (s, 1H, CH = N), 7.2–8.2 (m, 9H, Ar-H), 5.6–5.7 (d, 1H, pyran), 2.3–2.4 (s, 3H, CH_3). ^{13}CNMR (DMSO-d_6) δ: 171.52, 163.76, 155.61, 136.84, 133.77, 133.42, 131.08, 129.52, 129.25, 129.21, 128.96, 128.84, 128.81, 127.46, 126.93, 117.39, 76.52, 71.20, 49.05, 26.64, 14.71. MS (*m/z*): 376.91 [M + 1]. IR (KBr) cm^{-1}: 2160 (−CN), 2916, 2849 (Ar-CH).Anal. Calcd. For $C_{21}H_{15}ClN_4O$: C, 67.29; H, 4.03; Cl, 9.46; N, 14.96; O, 4.27. Found C, 67.23; H, 3.99; Cl, 9.42; O, 4.25.

4.4.4.5. 4-(4-fluorophenyl)-3-methyl-6-[{(1E)-(4-hydroxyphenyl) methylene}amino]-1,4-dihydro pyrano[2,3-c]pyrazole-5-carbonitrile (6e). The crude product was purified by eluting with mobile phase Hexane and AcOEt (70:30) affording 45% yield mp 185–187 °C; ^{1}HNMR (DMSO-d_6) δ: 7.2–8.2 (m, 8H, Ar-H), 10.2–10.8 (s, 1H, −OH), 8.8–9.1 (s, 1H, CH = N), 5.8–5.6 (d, 1H, pyran), 2.0–2.1 (s, 3H, CH_3).^{13}CNMR (DMSO-d_6) δ: 171.54, 163.71, 160.86, 160.24, 155.62, 134.81, 130.68, 130.62, 129.75, 129.71, 126.34, 117.38, 116.04, 116.01, 115.65, 115.60, 76.54, 71.22, 49.58, 26.61, 19.86. MS (*m/z*): 375.48 [M + 1]. IR (KBr) cm^{-1}: 2160 (−CN), 2916, 2849 (Ar-CH), 3230 (−OH).Anal. Calcd. For $C_{21}H_{15}FN_4O_2$: C, 67.37; H, 4.04; F, 5.07; N, 14.97; O, 8.55. Found C, 67.32; H, 4.06; F, 5.03; N, 14.93; O, 8.51.

4.4.4.6. 3-methyl-1,4-diphenyl-6-[{(1E)-phenylmethylene}amino]-1,4-dihydropyrano[2,3-c] pyrazole-5-carbonitrile (6f). The crude product was purified by eluting with mobile phase Hexane and AcOEt (70:30) affording 48% yield mp 160–162 ^{0}C.^{1}HNMR (DMSO-d_6) δ: 6.6–7.9 (m, 15H, Ar-H), 8.2–8.5 (s, 1H, CH = N), 4.2–4.3 (d, 1H, pyran), 1.9–2.0 (s, 3H, CH_3).^{13}CNMR (DMSO-d_6) δ: 171.54, 163.71, 155.62, 143.87, 139.22, 133.77, 131.05, 129.52, 129.50, 129.24, 129.21, 127.94, 128.87, 128.61, 128.56, 128.15, 128.11, 126.09, 120.83, 117.32, 116.77, 116.72, 85.81, 71.26, 46.95, 26.91, 20.15. MS (*m/z*): 417.53 [M + 1].IR (KBr) cm^{-1}: 2140 (−CN), 2900, 2815 (Ar-CH).Anal. Calcd. For $C_{27}H_{20}N_4O$: C, 77.87; H, 4.84;N, 13.45; O, 3.83. Found C, 77.84; H, 4.76; N, 13.41; O, 3.79.

4.4.4.7. 4-(4-hydroxyphenyl)-3-methyl-6-[{(1E)-phenylmethylene}amino]-1,4-dihydropyrano [2,3-c]pyrazole-5-carbonitrile (6 g). The crude product was purified by eluting with mobile phase Hexane and AcOEt (70:30) affording 42% yield mp 280–282 ^{0}C.^{1}HNMR (DMSO-d_6) δ: 6.9–7.9 (m, 14H, Ar-H), 3.8–3.9 (s, 1H, −OH), 8.6–8.7 (s, 1H, CH = N), 4.4–4.5 (d, 1H, pyran), 2.0–2.1 (s, 3H, CH_3). ^{13}CNMR (DMSO-d_6) δ: 171.48, 163.67, 158.60, 143.76, 139.35, 133.64, 131.11, 129.47, 129.42, 129.36, 129.17, 127.05, 128.63, 128.57, 128.44, 128.21, 128.05, 126.31, 120.78, 117.65, 116.42, 116.30, 85.68, 71.39, 46.82, 26.15, 20.02. MS (*m/z*): 433.62 [M + 1]. IR (KBr) cm^{-1}: 2170 (−CN), 2946, 2800 (Ar-CH).Anal. Calcd. For $C_{27}H_{20}N_4O_2$: C, 74.98; H, 4.66; N, 12.95; O, 7.40. Found C, 74.92; H, 4.62; N, 12.93; O, 7.35.

4.4.4.8. 6-[{(1E)-(4-hydroxyphenylmethylene}amino]-4-(4-methoxyphenyl)-3-methyl-1-phenyl-1,4-dihydropyrano[2,3-c]pyrazole-5-carbonitrile (6 h). The crude product was purified by eluting with mobile phase Hexane and AcOEt (70:30) affording 38% yield mp 215–218 ^{0}C.^{1}HNMR (DMSO-d_6) δ: 10.2–10.8 (s, 1H, OH), 6.9–7.9 (m, 14H, Ar-H), 10.2–10.8 (s, 1H, −OH), 8.6–8.7 (s, 1H, CH = N), 4.4–4.5 (d, 1H, pyran), 3.8–3.9 (s, 3H, CH_3). ^{13}CNMR (DMSO-d_6) δ: 169.82, 163.71, 160.84, 157.68, 153.95, 147.17, 137.52, 130.65, 130.61, 130.12, 130.07, 129.38, 129.31, 127.36, 126.39, 126.35, 126.21, 122.55, 122.51, 119.08, 116.04, 116.02, 114.28, 114.25, 77.96, 55.82, 26.35, 13.40. MS (*m/z*): 463.55 [M + 1]. IR (KBr) cm^{-1}: 2160 (−CN), 2900, 2875 (Ar-CH), 3190 (−OH).Anal. Calcd. For $C_{28}H_{22}N_4O_3$: C, 72.71; H, 4.79;N, 12.11; O, 10.38. Found C, 72.69; H, 4.75; N, 12.08; O, 10.35.

4.4.4.9. 4-(3,4-dimethoxyphenyl)-3-methyl-1-phenyl-6-[{(1E)-phenylmethylene}amino]-1,4-dihydropyrano[2,3-c]pyrazole-5-carbonitrile (6i). The crude product was purified by eluting with mobile phase Hexane and AcOEt (70:30) affording 32% yield mp 160–162 ^{0}C.^{1}HNMR (DMSO-d_6) δ: 9.1–9.0 (s, 1H, CH = N), 6.9–8.2 (m, 13H, Ar-H), 4.2–4.3 (d, 1H, pyran), 3.7–4.0 [d, 6H, $(OCH_3)_2$], 2.3–2.4 (s, 3H, CH_3). ^{13}CNMR (DMSO-d_6) δ: 169.78, 163.66, 157.54, 153.57, 149.72, 147.35, 137.58, 131.09, 130.42, 130.36, 130.18, 130.15, 129.57, 129.45, 127.19, 126.22, 126.28, 126.14, 122.69, 122.39, 119.16, 116.12, 116.05, 114.57, 77.68, 56.12, 55.75, 26.40, 13.58. MS (*m/z*): 475.32 [M − 1]. IR (KBr) cm^{-1}: 2150 (−CN), 2962, 2839 (Ar-CH).Anal. Calcd. For $C_{29}H_{24}N_4O_3$: C, 73.09; H, 5.08;N, 11.76; O, 10.07. Found C, 73.06; H, 5.04; N, 11.75; O, 10.05.

4.4.4.10. 6-[{(1E)-(4-hydroxyphenylmethylene}amino]-4-(3,4,5-trimethoxyphenyl)-3-methyl-1-phenyl-1,4-dihydropyrano[2,3-c]pyrazole-5-carbonitrile (6j). The crude product was purified by eluting with mobile phase Hexane and AcOEt (70:30) affording 40% yield mp 225–227 ^{0}C.^{1}HNMR (DMSO-d_6) δ: 9.8–10.0 (s, 1H, OH), 9.0–9.1 (s, 1H, CH═N), 7.6–7.7 (s, 1H, −OH), 6.6–8.2 (m, 11*H*, Ar-H), 4.1–4.4 (d, 1H, pyran), 3.5–3.9 [d, 6H, $(OCH_3)_2$], 1.9–2.0 (s, 3H, CH_3). ^{13}CNMR (DMSO-d_6) δ: 169.56, 163.72, 160.48, 157.38, 153.26, 149.39, 148.26, 147.55, 137.64, 130.58, 130.17, 130.09, 130.04, 129.51, 129.37, 127.28, 126.59, 126.34, 126.11, 122.54, 122.58, 119.08, 116.10, 116.24, 77.42, 56.22, 55.16, 55.69, 26.12, 13.45. MS (*m/z*): 523.47 [M + 1]. IR (KBr) cm^{-1}: 2210 (−CN), 2900, 2860 (Ar-CH), 3240 (−OH).Anal. Calcd. For $C_{30}H_{26}N_4O_5$: C, 68.95; H, 5.02;N, 10.72; O, 15.31. Found: C, 68.94; H, 4.98; N, 10.68; O, 15.25.

4.4.4.11. 4-(2-nitrophenyl)-3-methyl-1-phenyl-6-[{(1E)-phenylmethylene}amino]-1,4-dihydr opyrano[2,3-c]pyrazole-5-carbonitrile (6 k). The crude product was purified by eluting with mobile phase Hexane and AcOEt (70:30) affording 42% yield mp 210–212 ^{0}C.^{1}HNMR (DMSO-d_6) δ: 8.2–8.4 (s, 1H, CH = N), 7.1–7.9 (m, 14H, Ar-H), 4.4–4.6 (d, 1H, pyran), 1.8–2.0 (s, 3H, CH_3).^{13}CNMR (DMSO-d_6) δ: 169.82, 163.75, 153.98,149.31, 147.10, 137.54, 134.76, 133.73, 132.81, 131.09, 129.93, 129.36, 129.31, 129.28, 129.24, 128.82, 128.80, 126.66, 126.25, 124.81, 122.58, 122.48, 119.11, 117.35, 77.92, 21.75, 13.41. MS (*m/z*): 462.76 [M + 1]. IR (KBr) cm^{-1}: 2170 (−CN), 2900, 2845 (Ar-CH).Anal. Calcd. For $C_{27}H_{19}N_5O_3$: C, 70.27; H, 4.15; N, 15.18; O, 10.40. Found: C, 70.22; H, 4.11; N, 15.22; O, 10.35.

4.4.4.12. 4-(3-nitrophenyl)-3-methyl-1-phenyl-6-[{(1E)-phenylmethylene}amino]-1,4-dihydro pyrano[2,3-c]pyrazole-5-carbonitrile (6 l). The crude product was purified by eluting with mobile phase Hexane and AcOEt (70:30) affording 44% yield mp 145–147 ^{0}C.^{1}HNMR (DMSO-d_6) δ: 8.1–8.3 (s, 1H, CH = N), 7.1–7.9 (m, 14H, Ar-H), 4.4–4.6 (d, 1H, pyran), 2.0–2.1 (s, 3H, CH_3). ^{13}CNMR (DMSO-d_6) δ: 169.76, 163.55, 153.87, 149.27, 147.15, 137.48, 134.36, 133.56, 132.78, 131.24, 129.36, 129.16, 129.05, 129.00, 128.80, 128.64, 128.35, 126.42, 126.12, 124.45, 122.38, 122.18, 119.36, 117.14, 77.82, 21.52, 13.06. MS (*m/z*): 462.73 [M + 1]. IR (KBr) cm^{-1}: 2170 (−CN), 2900, 2845 (Ar-CH).Anal. Calcd. For $C_{27}H_{19}N_5O_3$: C, 70.27; H, 4.15;N, 15.18; O, 10.40. Found: C, 70.22; H, 4.11; N, 15.13; O, 10.36.

4.4.4.13. 4-(2-chlorophenyl)-3-methyl-1-phenyl-6-[{(1E)-phenylmethylene}amino]-1,4-dihydro pyrano[2,3-c]pyrazole-5-carbonitrile (6 m). The crude product was purified by eluting with mobile phase Hexane and AcOEt (70:30) affording 40% yield mp 120–122 ^{0}C.^{1}HNMR (DMSO-d_6) δ: 8.2–8.4 (s, 1H, CH = N), 7.2–8.2 (m, 14H, Ar-H), 5.6–5.7 (d, 1H, pyran), 1.6–1.8 (s, 3H, CH_3). ^{13}CNMR (DMSO-d_6) δ: 169.68, 163.42, 160.28, 153.28, 149.36, 147.01, 137.19, 134.21, 133.42, 132.60, 129.22, 129.09, 129.01, 128.86, 128.52, 128.31, 128.25, 126.11, 126.07, 124.54, 122.18, 122.06, 119.72, 117.28, 77.62, 21.08, 13.55. MS (*m/z*): 451.87 [M + 1]. IR (KBr) cm^{-1}: 2160 (−CN), 2916, 2849 (Ar-CH).Anal. Calcd. For $C_{27}H_{19}ClN_4O_2$: C, 69.45; H, 4.10; Cl, 7.59; N, 15.23; O, 6.85. Found: C, 69.42; H, 4.05; Cl, 7.56; N, 15.18; O, 6.82.

4.4.4.14. 6-[{(1E)-(4-hydroxyphenylmethylene}amino]-4-(3-chlorophenyl)-3-methyl-1-phenyl-1,4-dihydropyrano[2,3-c]pyrazole-5-carbonitrile (6n). The crude product was purified by eluting with mobile phase Hexane and AcOEt (70:30) affording 45% yield mp 178–180 °C.^{1}HNMR (DMSO-d_6) δ: 8.7–8.8 (s, 1H, OH), 8.6–8.7 (s, 1H, CH = N), 6.9–8.5 (m, 13H, Ar-H), 3.7–4.0 (d, 1H, pyran), 2.3–2.4 (s, 3H, CH_3). ^{13}CNMR (DMSO-d_6) δ: 169.56, 163.82, 161.72, 160.58, 153.18, 149.27, 147.11, 137.28, 134.90, 133.68, 129.36, 129.18, 129.08, 128.76, 128.68, 128.15, 128.34, 126.13, 126.42, 124.26, 122.58, 122.26, 119.69, 117.25, 77.16, 21.15, 13.08. MS (*m/z*): 466.85 [M +]. IR (KBr) cm^{-1}: 2160 (−CN), 2916, 2849 (Ar-CH), 3214 (−OH).Anal. Calcd. For $C_{27}H_{19}ClN_4O_2$: C, 69.45; H, 4.10; Cl, 7.59; N, 12.00; O, 6.85. Found: C, 69.42; H, 4.05; Cl, 7.55; N, 12.04; O, 6.78.

4.4.4.15. 6-[{(1E)-(4-hydroxyphenylmethylene}amino]-4-(4-fluorophenyl)-3-methyl-1-phenyl-1,4-dihydropyrano[2,3-c]pyrazole-5-carbonitrile (6o). The crude product was purified by eluting with mobile phase Hexane and AcOEt (70:30) affording 46% yield mp 206–208 °C.^{1}HNMR (DMSO-d_6) δ: 9.2–9.4 (s, 1H, OH), 7.1–7.9 (m, 13H, Ar-H), 8.7–8.8 (s, 1H, CH = N), 5.6–5.8 (d, 1H, pyran), 2.0–2.1 (s, 3H, CH_3). ^{13}CNMR (DMSO-d_6) δ: 169.32, 163.54, 161.68, 160.72,

153.24, 149.53, 147.16, 137.92, 134.85, 133.52, 129.18, 129.05, 129.00, 128.51, 128.16, 128.05, 128.01, 126.50, 126.24, 124.72, 122.63, 122.13, 119.58, 117.43, 77.15, 21.43, 13.87. MS (*m/z*): 451.33 [M + 1]. IR (KBr) cm^{-1}: 2160 (−CN), 2966, 2840 (Ar-CH), 3260 (−OH).Anal. Calcd. For $C_{27}H_{19}FN_4O_2$: C, 71.99; H, 4.25;F, 4.22;N, 12.44; O, 7.10. Found: C, 71.96; H, 4.22; F, 4.18; N, 12.42; O, 7.05.

5. Pharmacological studies

5.1. In vivo anti-inflammatory activity: Carrageenan induced rat paw edema model [19,38]

All the final compounds were screened for *in vivo* anti-inflammatory activity on albino rats of both sex weighing 150–200 g. Ibuprofen was taken as standard drug and including control, rats were divided to 18 groups with six from each group. All the compounds were administered orally by making 1% suspension in normal saline with gum acacia. After 30 min 0.1 ml of 1% carrageenan (supplied by Sigma Chemical Company, St. Louis, USA) suspension in normal saline was injected into the sub planar region of paw of each rat. Prior to study, all the animals were maintained in a restricted area in animal cages for a week. Animal laboratory was maintained at 25 ± 2 ^{0}C and relative humidity of 45–55%. After approval from ethical committee and observation, animals were adopted for screening. Food and water was not given to animals before 18 h of experiment. Edema volumes were measured for every hour up to 4 h in all the groups. All the values were recorded to calculate for mean edema volume and compared with toxicant carrageenan and standard. Percentage reduction for each compound was determined by substituting the values in the below formula.

$$\text{Percentage reduction} = \frac{V_0 - V_t}{V_0} \times 100$$

where V_0 = paw volume of control at respective time

V_t = paw volume of drug treated at respective time

5.2. Acute ulcerogenic studies

Acute Ulcerogenic studies were carried out for the most biologically active synthesized pyrazole derivatives **6 h, 6i, 6 k, 6 m** and **6o** and Ibuprofen as standard was evaluated using the previously reported procedure [39]. For the study, adult male albino rats weighing in the range of 120–150 g were selected and segregated into eight groups comprising of five animals each. All the rats were fasted for 20 h before administering the compounds for testing. The group one were administered 1% aqueous solution in tween 80 for control group. The other two groups were administered with Ibuprofen, aspirin and celecoxib respectively and were treated as reference drugs up to a dose of 100 mg/kg suspended in solution of 1% tween.

The other groups were given the active pyrazole derivatives (**6h, 6i, 6k, 6m** and **6o)** in a dose of 50 mg/kg suspended in 1% solution of tween. The compounds were administered once in a day for three consecutive days continuously to all the groups. After two hours of administration of last dose, all the rats were sacrificed using general anesthesia and the stomach was extracted, untied and washed with saline. Gastric mucosa was inspected with magnifying lens (10x) to check the sign of any lesions in the form of a hemorrhage, erosions or any breaks in the mucosal skin. The degree of ulcerogenic activity was calculated in terms of dividing the percentage of incidence of ulcers for all the groups of animals by 10, then the average of number of ulcers per stomach was scored visually based on the ulcer score to check the severity of the ulcer. The ulcer score is calculated based on 0 indicating no ulcer, mucosal erythema indicates 1, mild mucosal edema indicates score 2, and 3 indicates of moderate edema with bleeding ulcers and 4 indicates severe ulceration with edema, erosions and necrosis. The numbers and their sum indicates the toxicity of pyrazoles i.e., ulcer index.

5.3. Study of anti-inflammatory effect by membrane stabilizing property [40]

Alsever solution was prepared by 2% of dextrose, 0.8% of sodium citrate, 0.05% of citric acid and 0.42% of sodium chloride dissolving in distilled water. Solution was filtered and sterilized. Human blood was collected from a healthy volunteer and mixed with sterilized Alsever solution in equal volumes. Then tube was centrifuged at 3000 rpm for separation of cells. Supernatant liquid was removed and cells were washed with 1% (v/v) of isosaline. Different concentrations of EECR were prepared in mixture consisting 1 ml of phosphate buffer, 2 ml of hyposaline and 0.5 ml of HRBC suspension. Ibuprofen as standard drug and distilled water as control were used for the study. All the samples were placed in incubator at 37 ^{0}C for 30 min. After incubation, tubes were centrifuged, supernatant was collected and estimated for hemoglobin content at 560 nm using UV Spectrometer. All the readings were recorded for calculate the membrane stabilizing property of pyrazoles and standard drug with respect to control.

$$\%\text{Stabilizing activity} = 100 - \frac{\dfrac{\text{Absorbance of drug}}{\text{treated sample}} - \text{Absorbance of control 2}}{\text{Absorbance of control 1}} \times 100$$

5.4. In vitro cyclooxygenase inhibitor assay

All the synthesized pyrazole derivatives were screened for *in vitro* evaluation of both COX-1 & COX-2 enzyme inhibition assay to determine the COX-2 inhibition potential and Selectivity Index (SI) and to investigate the SAR. All the test compounds were prepared dilutions in the range of 0.03–300 μM. Selective COX-2 inhibitor, Celecoxib was used as standard and prepared dilutions in the range of 0.03–3.00 μM for COX-2 and 0.03–50 μM for COX-1. The assay was performed using COX inhibitor Screening Assay Kit (Catalog No. 560131, Cayman Chemical, Ann Arbor, MI, USA). Method works on the principle of Enzyme Immunoassay (EIA) using ovine COX-1 and human recombinant COX-2 enzymes. Inhibition potential of compounds was calculated by incubating reaction buffer, heme, respective COX-1 or COX-2 enzyme with test compound or standard for 10 min at 37 ^{0}C. Later the reaction was allowed to initiate by the addition of arachidonic acid and continued incubation for 2 more minutes at 37 ^{0}C. Enzyme function was terminated by the addition of hydrochloric acid. Further addition of stannous chloride ($SnCl_2$) allows the reduction reaction of prostaglandin H2 (PGH2) to PGF2α catalyzed by COX enzyme. Quantification of PGF2α using the assay kit provided the COX inhibition potential of compounds. All the solutions containing PGF2α were diluted and transferred to pre-coated 96 well plates with monoclonal anti-rabbit IgG antibodies of mouse. Plates were incubated for overnight with PG-acetylcholinesterase (AchE) conjugate and specific prostaglandin antiserum. Later the solution and other unbound reagents were removed with micropipette, washed the wells and added Ellman's reagent (containing AchE substrate). Allowed for 1 h incubation and yellow colored product obtained by AchE reaction was measured using ELISA reader at 412 nm. Assay protocol was followed as per the instructions of kit manufacturer and found color intensity was inversely proportional to prostaglandin concentration [30–33]. All the dilutions of test compounds and standard were taken in duplicate and IC_{50} values were calculated from sigmoidal curve.

Acknowledgements

The authors are thankful to Shri Vile Parle Kelavani Mandal's, NMIMS, Mumbai and M.S. Ramaiah University of Applied Sciences, Bangalore for providing the necessary facilities to carry out this research work. Authors are also extending their thanks to Chairman of Star Tech Hyderabad and Astra Zeneca Bangalore for providing spectral data.

Conflict of Interest

The authors confirm that this article content has no conflicts of interest.

Appendix A. Supplementary material

Supplementary data to this article can be found online at https://doi.org/10.1016/j.bioorg.2019.02.031.

References

[1] M. Drini, Peptic ulcer disease and non-steroidal anti-inflammatory drugs, Aust. Prescr. 40 (2017) 91–93, https://doi.org/10.18773/austprescr.2017.037.
[2] W.H. Hörl, Nonsteroidal anti-inflammatory drugs and the kidney, Pharmaceuticals (Basel). 3 (2010) 2291–2321, https://doi.org/10.3390/ph3072291.
[3] R.I. Russell, Non-steroidal anti-inflammatory drugs and gastrointestinal damage-problems and solutions, Postgrad. Med. J. 77 (2001) 82–88, https://doi.org/10.1136/PMJ.77.904.82.
[4] L.M. Jackson, Cyclooxygenase (COX) 1 and 2 in normal, inflamed, and ulcerated human gastric mucosa, Gut. 47 (2000) 762–770, https://doi.org/10.1136/gut.47.6.762.
[5] A. Whelton, C.W. Hamilton, Nonsteroidal anti-inflammatory drugs: effects on kidney function, J. Clin. Pharmacol. 31 (1991) 588–598, https://doi.org/10.1002/j.1552-4604.1991.tb03743.x.
[6] D.S. Dogruer, E. Kupeli, E. Yesilada, M.F. Sahin, Synthesis of new 2-[1(2H)-phthalazinon-2-yl]-acetamide and 3-[1(2H)-phthalazinon-2-yl]-propanamide derivatives as antinociceptive and anti-inflammatory agents, Arch. Pharm. (Weinheim) 337 (2004) 303–310, https://doi.org/10.1002/ardp.200200719.
[7] K. Karrouchi, S. Radi, Y. Ramli, J. Taoufik, Y. Mabkhot, F. Al-aizari, M. Ansar, Synthesis and pharmacological activities of pyrazole derivatives: a review, Molecules 23 (2018) 134, https://doi.org/10.3390/molecules23010134.
[8] A. Ansari, A. Ali, M. Asif, S. Shamsuzzaman, Review: biologically active pyrazole derivatives, New J. Chem. 41 (2017) 16–41, https://doi.org/10.1039/C6NJ03181A.
[9] Y.-R. Li, C. Li, J.-C. Liu, M. Guo, T.-Y. Zhang, L.-P. Sun, C.-J. Zheng, H.-R. Piao, Synthesis and biological evaluation of 1,3-diaryl pyrazole derivatives as potential antibacterial and anti-inflammatory agents, Bioorg. Med. Chem. Lett. 25 (2015) 5052–5057, https://doi.org/10.1016/J.BMCL.2015.10.028.
[10] S.A.H. El-Feky, Z.K. Abd El-Samii, N.A. Osman, J. Lashine, M.A. Kamel, H.K. Thabet, Synthesis, molecular docking and anti-inflammatory screening of novel quinoline incorporated pyrazole derivatives using the Pfitzinger reaction II, Bioorg. Chem. 58 (2015) 104–116, https://doi.org/10.1016/J.BIOORG.2014.12.003.
[11] B.M. Chougala, S. Samundeeswari, M. Holiyachi, L.A. Shastri, S. Dodamani, S. Jalalpure, S.R. Dixit, S.D. Joshi, V.A. Sunagar, Synthesis, characterization and molecular docking studies of substituted 4-coumarinylpyrano[2,3-c]pyrazole derivatives as potent antibacterial and anti-inflammatory agents, Eur. J. Med. Chem. 125 (2017) 101–116, https://doi.org/10.1016/J.EJMECH.2016.09.021.
[12] M.M. Mohy El-Din, A.M. Senbel, A.A. Bistawroos, A. El-Mallah, N.A. Nour El-Din, A.A. Bekhit, H.A. Abd El Razik, A novel COX-2 inhibitor pyrazole derivative proven effective as an anti-inflammatory and analgesic drug, Basic Clin. Pharmacol. Toxicol. 108 (2011) 263–273, https://doi.org/10.1111/j.1742-7843.2010.00648.x.
[13] S. Maddila, S. Gorle, C. Sampath, P. Lavanya, Synthesis and anti-inflammatory activity of some new 1,3,4-thiadiazoles containing pyrazole and pyrrole nucleus, J. Saudi Chem. Soc. 20 (2016) S306–S312, https://doi.org/10.1016/j.jscs.2012.11.007.
[14] K.R.A. Abdellatif, E.K.A. Abdelall, W.A.A. Fadaly, G.M. Kamel, Synthesis, cyclooxygenase inhibition, and anti-inflammatory evaluation of novel diarylheterocycles with a central pyrazole, pyrazoline, or pyridine ring, Med. Chem. Res. 24 (2015) 2632–2644, https://doi.org/10.1007/s00044-015-1327-7.
[15] M.L. Capone, S. Tacconelli, M.G. Sciulli, P. Patrignani, Clinical pharmacology of selective COX-2 inhibitors, Int. J. Immunopathol. Pharmacol. 16 (2003) 49–58 (accessed January 1, 2019), http://www.ncbi.nlm.nih.gov/pubmed/14552704.
[16] A. Zarghi, S. Arfaei, Selective COX-2 inhibitors: a review of their structure-activity relationships, Iran. J. Pharm. Res. 10 (2011) 655–683, https://doi.org/10.1093/humrep/12.10.2313.
[17] A. Gürsoy, Ş. Demirayak, G. Çapan, K. Erol, K. Vural, Synthesis and preliminary evaluation of new 5-pyrazolinone derivatives as analgesic agents, Eur. J. Med. Chem. 35 (2000) 359–364, https://doi.org/10.1016/S0223-5234(00)00117-3.
[18] G. Turan-Zitouni, M. Sivaci, F.S. Kiliç, K. Erol, Synthesis of some triazolyl-antipyrine derivatives and investigation of analgesic activity, Eur. J. Med. Chem. 36 (2001) 685–689, https://doi.org/10.1016/S0223-5234(01)01252-1.
[19] T.M.A. Elmaati, Reactions with heterocyclic amidines: new routes for the synthesis of novel azolo[1,5-, Acta Chim. Slov. 49 (2002) 13–15.
[20] M.M.F. Ismail, Y.A. Ammar, H.S.A. El-Zahaby, S.I. Eisa, S. El-Sayed Barakat, Synthesis of novel 1-pyrazolylpyridin-2-ones as potential anti-inflammatory and analgesic agents, Arch. Pharm. (Weinheim). 340 (2007) 476–482, https://doi.org/10.1002/ardp.200600197.
[21] F.F. Fleming, L. Yao, P.C. Ravikumar, L. Funk, B.C. Shook, Nitrile-containing pharmaceuticals: efficacious roles of the nitrile pharmacophore, J. Med. Chem. 53 (2010) 7902–7917, https://doi.org/10.1021/jm100762r.
[22] J.R. Vane, R.M. Botting, Mechanism of action of anti-inflammatory drugs: an overview, Sel. COX-2 Inhib. Springer Netherlands, Dordrecht, 1998, pp. 1–17, , https://doi.org/10.1007/978-94-011-4872-6_1.
[23] R.N. Dubois, S.B. Abramson, L. Crofford, R.A. Gupta, L.S. Simon, L.B.A. Van De Putte, P.E. Lipsky, Cyclooxygenase in biology and disease, FASEB J. 12 (1998) 1063–1073, https://doi.org/10.1096/fasebj.12.12.1063.
[24] C.S. Williams, M. Mann, R.N. Dubois, The role of cyclooxygenases in inflammation, cancer, and development, Cancer. 18 (1999) 7908–7916 (accessed September 8, 2018), https://www.nature.com/articles/1203286.
[25] M. Nivsarkar, M. Mukherjee, M. Patel, H. Padh, C. Bapu, Launaea nudicaulis leaf juice exhibits anti inflammatory action in acute and chronic inflammation models in rats, Indian Drugs. 39 (2002) 290–292.
[26] O.A. Olajide, J.M. Makinde, D.T. Okpako, S.O. Awe, Studies on the anti-inflammatory and related pharmacological properties of the aqueous extract of Bridelia ferruginea stem bark, J. Ethnopharmacol. 71 (2000) 153–160, https://doi.org/10.1016/S0378-8741(99)00201-9.
[27] S. Kalaiselvan, M.K. Rasool, The anti-inflammatory effect of triphala in arthritic-induced rats, Pharm. Biol. 53 (2015) 51–60, https://doi.org/10.3109/13880209.2014.910237.
[28] A. Bag, S. Kumar Bhattacharyya, N. Kumar Pal, R.R. Chattopadhyay, Anti-inflammatory, anti-lipid peroxidative, antioxidant and membrane stabilizing activities of hydroalcoholic extract of Terminalia chebula fruits, Pharm. Biol. 51 (2013) 1515–1520, https://doi.org/10.3109/13880209.2013.799709.
[29] M.A.-A. El-Sayed, N.I. Abdel-Aziz, A.A.-M. Abdel-Aziz, A.S. El-Azab, Y.A. Asiri, K.E.H. ElTahir, Design, synthesis, and biological evaluation of substituted hydrazone and pyrazole derivatives as selective COX-2 inhibitors: Molecular docking study, Bioorg. Med. Chem. 19 (2011) 3416–3424, https://doi.org/10.1016/j.bmc.2011.04.027.
[30] M.A.-A. El-Sayed, N.I. Abdel-Aziz, A.A.-M. Abdel-Aziz, A.S. El-Azab, K.E.H. ElTahir, Synthesis, biological evaluation and molecular modeling study of pyrazole and pyrazoline derivatives as selective COX-2 inhibitors and anti-inflammatory agents, Part 2, Bioorg. Med. Chem. 20 (2012) 3306–3316, https://doi.org/10.1016/j.bmc.2012.03.044.
[31] Schrödinger Release 2018-3: LigPrep, Schrödinger, LLC, New York, NY, 2018, (n.d.).
[32] Small-Molecule Drug Discovery Suite 2018-3, Schrödinger, LLC, New York, NY, 2018., (n.d.).
[33] Schrödinger Release 2018-3: Maestro, Schrödinger, LLC, New York, NY, 2018, (n.d.).
[34] Schrödinger Release 2018-3: Phase, Schrödinger, LLC, New York, NY, 2018, (n.d.).
[35] R. Busse, I. Fleming, Pulsatile stretch and shear stress: Physical stimuli determining the production of endothelium-derived relaxing factors, J. Vasc. Res. 35 (1998) 73–84, https://doi.org/10.1021/jm5004914.
[36] Schrödinger Release 2018-3: AutoQSAR, Schrödinger, LLC, New York, NY, 2018, (n.d.).
[37] R. Parajuli, J. Banerjee, H. Khanal, Synthesis of some pyrazolone derivatives and evaluation of its antibacterial and cytotoxic activity, Orient. J. Chem. 31 (2015) 2099–2106, https://doi.org/10.13005/ojc/310430.
[38] O.a. Olajide, S.O. Awe, J.M. Makinde, Effect of the aqeous extract of Bridelia ferruginea stem bark on carrageenan-induced edema and granuloma tissue formation in rats and mice, J Ethnopharmacol. 66 (1999) 113–117, https://doi.org/10.1016/S0378-8741(99)00006-9.
[39] G.S. Hassan, S.M. Abou-Seri, G. Kamel, M.M. Ali, Celecoxib analogs bearing benzofuran moiety as cyclooxygenase-2 inhibitors: design, synthesis and evaluation as potential anti-inflammatory agents, Eur. J. Med. Chem. 76 (2014) 482–493, https://doi.org/10.1016/j.ejmech.2014.02.033.
[40] C.A. Anosike, O. Obidoa, L.U. Ezeanyika, Membrane stabilization as a mechanism of the anti-inflammatory activity of methanol extract of garden egg (Solanum aethiopicum), DARU J. Pharm. Sci. 20 (2012) 76, https://doi.org/10.1186/2008-2231-20-76.